Sequence, age, and source of silicic fallout tuffs in middle to late Miocene basins of the northern Basin and Range province

Michael E. Perkins*
Francis H. Brown
William P. Nash
Department of Geology and Geophysics, University of Utah, Salt Lake City, Utah 84112

William McIntosh
New Mexico Bureau of Mines and Mineral Resources, Socorro, New Mexico, 87801

S. K. Williams†
Department of Geology and Geophysics, University of Utah, Salt Lake City, Utah 84112

ABSTRACT

The latest Cenozoic (<6 Ma) ash beds in the western United States have been intensively studied for several decades. The more widespread of these ash beds are well-documented event horizons that are of great value in studies of the timing and pace of geological, climatological, and biological events throughout the region. Because explosive volcanism was not restricted to latest Neogene time in this region, many older ash beds are likely to prove as useful as younger beds as event horizons, once they are located, characterized, and dated. As a first step in developing a useful chronology of older Cenozoic ash beds in the western United States, we have sampled and analyzed silicic fallout tuffs in middle to late Miocene sedimentary basins across the northern Basin and Range province.

The northern Basin and Range basins, ideally situated in the vicinity of major coeval silicic volcanic centers, contain numerous relatively unaltered, silicic fallout tuffs. We have correlated tuffs between all sampled sections on the basis of glass shard composition. The composite stratigraphic sequence established by the correlations contains more than 200 individual tuffs, including 59 widely distributed tuffs termed correlative tuffs. The tuffs vary widely in composition, but most are in one of two compositional groups: gray metaluminous vitric tuffs (Gm tuffs) or white metaluminous vitric tuffs (Wm tuffs). Distribution patterns, compositional characteristics, and correlation with ash-flow tuffs show that the source for most Gm tuffs was the Snake River Plain volcanic province along the northern edge of the northern Basin and Range, and the source for most Wm tuffs was the southwestern Nevada volcanic field in the southern part of the northern Basin and Range.

The northern Basin and Range tuffs range in age from ca. 16–6 Ma. The ages of individual tuffs are determined variously by direct isotopic dating, by correlation to previously dated fallout and ash-flow tuffs, or by interpolation age estimation. Ages for most tuffs are known to within 0.25 m.y. (1σ) or less and for many tuffs to within 0.1 m.y. or less. The sequence and ages of tuffs established in this study provide insights into the evolution of the northern Basin and Range basins and patterns of explosive volcanism in coeval volcanic centers, and contribute to the development of a high-resolution stratigraphy and chronology of coeval sedimentary deposits throughout the western United States.

INTRODUCTION

Tephrochronology, the characterization, correlation, and age calibration of ash beds, has contributed substantially to our knowledge of the stratigraphy and chronology of latest Neogene sedimentary strata in the western United States (Izett, 1981; Sarna-Wojcicki and Davis, 1991). Of particular importance in tephrochronology are the widespread ash beds produced during major silicic volcanic eruptions. Such ash beds, including the well-known Mazama, Bishop, and Huckleberry Ridge ash beds, among others, commonly extend 1000–2000 km from source volcanoes and provide precise correlation and dating of latest Neogene sedimentary strata over large portions of the region.

In the western United States major explosive silicic volcanic eruptions occurred throughout the Cenozoic Era (Christiansen and Yeats, 1992). Hence, tephrochronology has the potential to provide the same precise long-distance correlation and dating of ash beds in older Cenozoic strata as we now have for ash beds in latest Neogene strata. With this goal in mind, we sampled sequences of silicic fallout tuffs in Miocene sedimentary basins of the northern Basin and Range province that were ideally situated to receive fallout ash from explosive eruptions in the coeval silicic volcanic centers of the region (Fig. 1). Building on pioneering studies of silicic tuffs of the northern Basin and Range basins (Van Houten, 1956; Eastwood, 1969; Smith, 1975; Smith and Nash, 1976; and Metcalf, 1982), we correlate tuffs across the northern Basin and Range and establish a composite sequence of 213 tuffs ranging in age from 16–6 Ma. We date this sequence by new $^{40}Ar/^{39}Ar$ laser-fusion dating of 7 tuffs, by correlation to 15 previously dated tuffs, and by linear interpolation between these dated tuffs. This well-characterized age-calibrated sequence of fallout tuffs has led to an improved understanding of the age of the northern Basin and Range basins, of rates of sediment accumulation in these basins, and of the frequency and timing of explosive eruptions in two important silicic volcanic centers that produced many of the tuffs preserved in these basins. The fallout-tuff record is an important resource for geologic research in the northern Basin and Range and adjacent regions of the western United States.

*e-mail: mperk@mines.utah.edu
†Present address: Southland Geotechnical, 242 North Eighth Street, El Centro, California 92243.

GSA Bulletin; March 1998; v. 110; no. 3; p. 344–360; 6 figures; 10 tables.

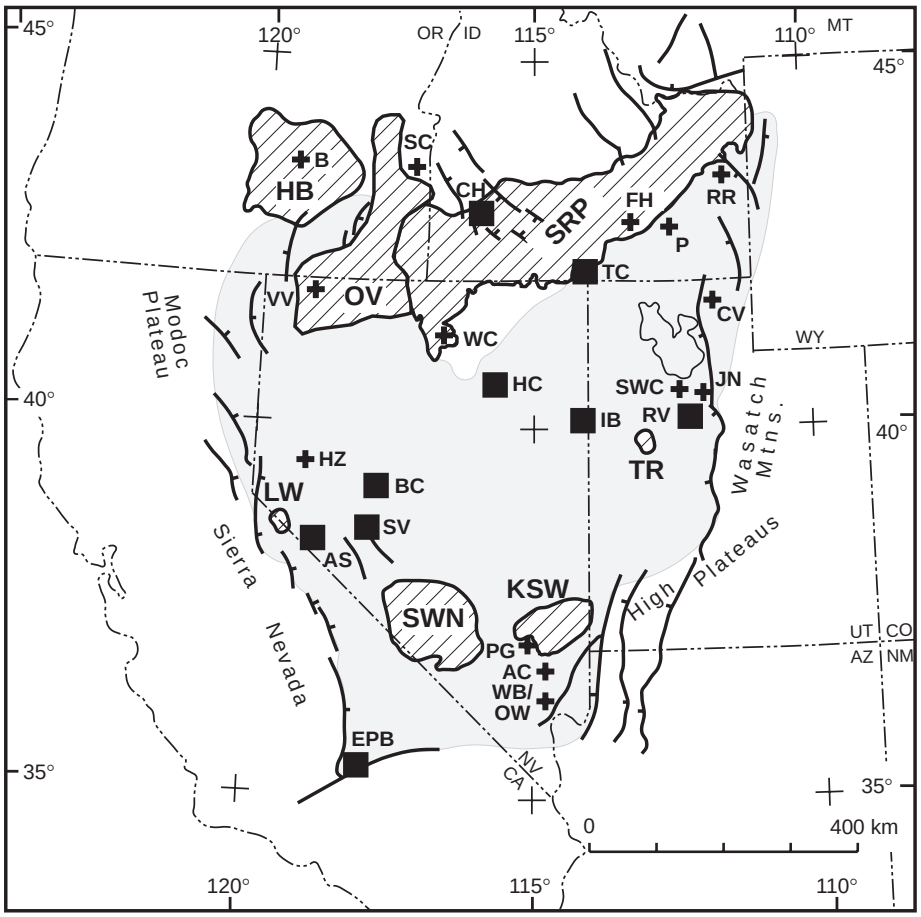

Figure 1. Location map showing principal sections (solid rectangles), ancillary sections (crosses), and major centers of middle to late Miocene explosive silicic volcanism (diagonal lined areas) within and around the northern Basin and Range province (shaded gray). Principal sections are: AS—Aldrich Station; BC—Buffalo Canyon; CH—Chalk Hills; EPB—El Paso basin; HC—Huntington Creek; IB—Ibapah Badlands; RV—Rush Valley; SV—Stewart Valley; and TC—Trapper Creek. Ancillary sections are: AC—Arrow Canyon; B—Burns; CV—Cache Valley; FH—Ferry Hollow; HZ—Hazen quarries; JN—Jordan Narrows; OW—Overton Wash; P—Pocatello; PG—Pahranagat Valley; RR—Ririe Reservoir; SC—Succor Creek; SWC—South Willow Canyon; VV—Virgin Valley and Thousand Creek; WB—White Basin; and WC—Willow Creek. Miocene centers of explosive silicic volcanism are: HB—Harney basin (10-5 Ma); KSW—Kane Spring Wash caldera complex (16–14 Ma); LW—Little Walker volcanic center (10–9 Ma); OV—"Orevada" volcanic province (16.5–15 Ma); SRP—Snake River Plain volcanic province (15–5 Ma, progressively younger to the northeast); SWN—southwestern Nevada volcanic field (16–7 Ma); TR—Thomas Range (7–6 Ma). Figure modified from Christiansen and Yeats (1992) and Luedke and Smith (1981, 1982, 1983).

LABORATORY AND FIELD METHODS

Glass Shard Analyses

About 700 samples of vitric tuffs were collected in this study. Glass shards from all samples were analyzed on a Cameca SX-50 electron probe at the University of Utah under analytical conditions described by Nash (1992). Typically, 20 shards per sample were analyzed. Estimates of H_2O content in the hydrated glass shards were calculated from the difference between measured and stoichiometric oxygen content as discussed by Nash (1992). Glass separates (≥99.5% glass) from ~350 samples collected in this study along with 210 glass separates originally analyzed by Eastwood (1969), Smith (1975), and Brown (1986) were analyzed for this study with an ARL 8410 X-ray fluorescence (XRF) spectrometer at the University of Utah using methods described in Perkins et al. (1995b).

$^{40}Ar/^{39}Ar$ Analyses

$^{40}Ar/^{39}Ar$ analyses of sanidine crystals were done for nine samples. The location and the stratigraphic position of these samples are in given Appendix A. Sanidine crystals were concentrated from the samples using standard techniques, and final separates of ~100 sanidine crystals were hand-picked from the concentrates. Prior to analysis the sanidines were treated with 5 % HF in an ultrasonic bath for 10–30 min to remove adhering glass. Aliquots of the sanidine separates were packaged with alternating flux monitors of Fish Canyon sanidine (27.84 Ma relative to MMhb–1 at 520.4 Ma; Sampson and Alexander, 1987) for irradiation. For coarser samples (sanidines 0.5–1.0 mm), single crystals were fused for isotopic analysis; for finer samples, small groups of sanidine crystals were fused for analysis. $^{40}Ar/^{39}Ar$ analyses were done at the New Mexico Geochronology Research Laboratory of the New Mexico Institute of Mining and Technology using instrumentation and methods described in Gregory and McIntosh (1996).

Section Measurements and Sampling Procedures

Field work included measurement of sections and collection of vitric tuff samples. Geologic mapping was done in areas extensively disrupted by faulting (e.g., Ibapah Badlands) to ensure that a complete section was sampled and that the positions of faults were accurately located. Thickness measurements were done with a Jacob's staff in most sections. Precision, based on duplicate measurements of several sections, is on the order of ±5% (±1σ). Two sections, the Aldrich Station section and the upper half of the El Paso basin section, are thick homoclinal sequences with widely spaced tuff beds. For these sections bedding orientation and sample location data were plotted on 7.5′ quadrangle maps and thickness was measured from cross sections constructed along the sampling traverses.

We sampled most visible vitric tuffs in the sections, collecting ~500 cm^3 from each sampled bed. When feasible, we avoided sampling parts of tuff beds that had obvious detrital contamination. For extensively reworked tuffs, it was usually necessary to search along the outcrop to locate a pocket of relatively uncontaminated tuff for sampling. Where tuffs were partly altered to zeolite or opal, a search along the bed usually revealed an area where alteration was minimal or absent.

STANDARDIZATION OF $^{40}Ar/^{39}Ar$ DATES

Our chronologic calibration of the vitric tuff sequence is based primarily on laser-fusion $^{40}Ar/^{39}Ar$ dates of sanidine reported from the Geochronology Laboratory of the U.S. Geological Survey, Menlo Park, California, the Berkeley Geochronology Center, Berkeley, California; and the New Mexico Geochronology Research Laboratory, Socorro, New Mexico. As discussed in Appendix B, ages assigned to Ar monitors differ between the Menlo Park laboratory and the other two laboratories by small but significant amounts. To compensate for these differences we increase ages reported by Menlo Park laboratory by a factor of 1.0105. When we refer to Menlo Park laboratory dates in the text we give the recalculated age followed parenthetically by the originally reported age. For example, Sawyer et al. (1994) reported an age of 11.60 ± 0.05 Ma for the Rainier Mesa Tuff, an ash-flow tuff that we correlate with a fallout tuff. In the text we give this age as 11.72 (11.60) ± 0.05 Ma (Sawyer et al., 1994).

TERMINOLOGY

Many fallout tuffs and reworked fallout tuffs described in this report are consolidated or cemented, so they can properly be termed tuffs. However, we often need to distinguish between a fallout tuff layer and a proximal ash-flow tuff unit produced during the same eruption. To do this we use the term "ash bed" when referring to an individual named fallout tuff. For example, the Rainier Mesa ash bed refers to a fallout tuff layer produced by the same eruption that generated the Rainier Mesa Tuff. When not referring to an individual fallout tuff layer we continue to use the descriptively more correct terms "tuff," "fallout tuff," and "vitric tuff."

DESCRIPTION OF SECTIONS

The vitric tuffs discussed here are from 25 areas (Fig. 1) in which either principal or ancillary sections were sampled and measured. The sequences of vitric tuffs established in the nine principal sections and the correlations between these sections provide a foundation for the sequence and age of middle to late Miocene vitric tuffs in the northern Basin and Range province. The principal sections, which are the most intensively sampled, generally have the best exposures and most comprehensive vitric tuff record. Vitric tuffs in the 16 ancillary sections (Fig. 1) provide chronological control not available from the principal sections or provide information about the areal distribution of some important vitric tuffs. Some essential information for all the sections is listed in Table 1 and section locations are described in Appendix A.

CHARACTERISTICS OF THE TUFFS

Physical Appearance

In the field we divided the vitric tuffs into three groups: gray vitric tuffs (67%), white biotitic tuffs (21%), and various other tuffs, often brownish-gray, termed dacite vitric tuffs (12%). The thickness of these tuffs ranges from less than 1 cm to 18 m. This extreme variation reflects a complex interplay of differences in eruption volume and duration, patterns of downwind distribution of the original ash cloud, fluvial and eolian reworking of fallout ash after deposition, and distance to source. Normally the thickest tuffs are the gray vitric tuffs and the thinnest are the dacite tuffs. The vitric tuffs typically consist of >90% glass shards. The median shard size for most tuffs is in the fine to very fine sand size range. Lapilli tuffs are rare, and some of the thinner tuffs have a median shard size in the coarse silt range. Glass shards in the gray vitric tuffs commonly have bubble-wall morphologies, although pumiceous morphologies are not uncommon. Pumiceous shards dominate in the white biotitic tuffs and the dacite tuffs.

The mineralogy of the tuffs has not been assessed in detail, but clear differences in the mafic minerals are noted between the major groups. In the gray vitric tuffs, mafic minerals are generally present in only trace amounts and consist primarily of clinopyroxene and, less commonly, hypersthene. Biotite ± hornblende is notably absent in all but a few of the gray vitric tuffs. In the white biotitic tuffs, biotite commonly comprises several percent of the tuff. In addition, a smaller amount of hornblende ± pyroxene is present in many of the white biotitic tuffs. In the dacite tuffs, hornblende ± pyroxene are generally present in amounts up to several percent, while biotite is uncommon. Both the gray vitric tuffs and white biotitic tuffs commonly contain quartz and feldspar; sanidine comprises a substantial proportion (>20%) of the feldspar in many of these tuffs. In contrast, quartz and sanidine are generally absent in the dacite tuffs, and plagioclase is the dominant felsic mineral.

The vitric tuffs, like the other associated sedimentary rocks, are generally friable to somewhat indurated. Indurated tuffs are typically calcite cemented or contain considerable amounts of secondary matrix material, primarily clay. Zeolitic alteration of the tuffs is uncommon, but some tuffs low in the El Paso basin, Willow Creek, and Succor Creek sections have been extensively or completely altered to zeolite ± clay ± opal, and a few tuffs at the base of the Buffalo Canyon section have glass shards that are partly replaced by zeolite. Opal coating of shard surfaces is characteristic of tuffs in the White Basin section and oc-

TABLE 1. SUMMARY INFORMATION FOR SAMPLED SECTIONS

Section	Units	Thickness (m)*	Age (Ma)†	Key reference
PRINCIPAL SECTIONS				
Aldrich Station	Wassuk Group	1900	9–13	Golia and Stewart (1984)
Buffalo Canyon	Buffalo Canyon Fm.	370	15.6 (base)	Axelrod (1991)
Chalk Hills	Chalk Hills Fm.	60	8.5–6.6	Kimmel (1982)
El Paso basin	Dove Spring Fm.	1280	13.5–7.3	Whistler and Burbank (1992)
Huntington Creek	Humboldt Fm	500+	~16–~9	Smith and Ketner (1976)
Ibapah Badlands	Salt Lake Fm.	450	~9 (top)	Heylmun (1965, p. 20)
Rush Valley	Salt Lake Fm.	350	——	Heylmun (1965, p. 19)
Stewart Valley	Stewart Valley Group	800	16–11.7	Shorn et al. (1989)
Trapper Creek	Idavada Group	930	13.9–8.6	Perkins et al. (1995b)
ANCILLARY SECTIONS				
Arrow Canyon	Muddy Creek Fm.	45	7.2–5.9	Metcalf (1982)
Burns	Rattlesnake Tuff	——	7.05	Streck and Grunder (1995)
Ferry Hollow	Walcott Tuff	——	6.4	Stearns and Isotoff (1956)
Hazen	Truckee Fm.	105	9.8 (base)	Lenz and Morris (1993)
Cache Valley, UT	Salt Lake Fm.	——	——	Hintze (1988, section 16)
Jordan Narrows, UT	Salt Lake Fm.	——	6.5	Naeser et al. (1983)
Pocatello, ID	Starlight Fm.	——	——	Trimble (1976)
Overton Wash	Thumb Member	150	17–14	Bohannon (1984)
Ririe Reservoir	Heise volcanic field	——	——	Hackett and Morgan (1988)
Paranagat Valley	Muddy Creek Fm.	60	8	Metcalf (1982)
S. Willow Canyon	Salt Lake Fm.	700	——	Hintze (1988, section 27)
Succor Creek	Sucker Creek Fm.	230	15.5–14.9	Downing (1992)
Thousand Creek	Thousand Creek Fm.	(60)	~8	Wendell (1970)
Virgin Valley	Virgin Valley Fm.	(450)	16–15	Greene (1984).
White Basin	Red sandstone unit	180+	12–10.5	Bohannon (1984)
White Basin	Lovell Wash Member	150	13.7–12	Bohannon (1984)
Willow Creek	Ttsl of Coats (1987)	120+	<32	Overlies Tt_2 of Coats (1987)

*Values in parentheses are those reported by other workers, otherwise from this study.
†Previously reported ages including: isotopic age dates; age estimates of mammalian faunas; magnetochronology; tephrochronology.

curs on shards in some tuffs in the basal part of the El Paso Basin section. Neither zeolitic minerals nor opal can generally be removed from glass, so the composition of glass from such tuffs was determined only by electron probe analysis.

Glass Composition

The 213 tuffs beds identified in the principal and ancillary sections show wide variation in glass shard compositions (Tables 2 and 3), allowing one tuff bed to be distinguished from another. Variation in glass composition is not completely random, however, and most vitric tuffs are within one of four broad compositional groups: (1) gray metaluminous rhyolite tuffs (Gm tuffs); (2) white metaluminous rhyolite tuffs (Wm tuffs); (3) dacite tuffs; and (4) gray peralkaline rhyolite tuffs (Gp tuffs), in order of relative abundance. The gray vitric tuffs of field terminology are mostly Gm tuffs along with some Gp and dacite tuffs. The white biotitic tuffs of field terminology are mostly Wm tuffs but include a few dacite tuffs, and the dacite tuffs of the field are mostly tuffs with a dacite glass composition.

Classification into one of these four compositional groups is based on content of Al, Fe, and Ca in glass shards (Fig. 2). Because of postdepositional changes in the Na and K content of glass shards and Na loss under the electron beam of the microprobe, the alkalies are not used in classification. Hence, classification as metaluminous or peralkaline is inferential. Gp tuffs contain glass having the lowest Ca and Al content and moderate to high Fe content. Gm tuffs contain glass having somewhat higher Al, higher Ca content, and a range in Fe content similar to that of the Gp tuffs. Wm tuffs contain glass having a moderate Al content, a low Fe content and consistently lower Fe/Al and Fe/Ca ratios than those of Gp tuffs. Dacite tuffs contain glass having the highest Al content and moderate to high Fe and Ca contents.

Other elements also show differences between major groups (Table 3). Gm and Gp tuffs generally have the highest contents of light rare earth elements (Ce > 90 ppm), the Gp tuffs being distinguished by very low contents of Ba (<20 ppm) and Sr (<5 ppm). Wm and dacite tuffs are characterized by lower contents of light rare earth elements (Ce < 90 ppm); Sr contents are lower in the Wm tuffs (<100 ppm) and higher in the dacite tuffs (>100 ppm). The Gm tuffs generally correspond to the G-type (gray-type) rhyolitic glasses described by Izett (1981), though the more Ca rich of the Gm tuffs extend, without compositional break, into Izett's field of dacitic glasses (Ca > 0.55 wt% or CaO > 0.77 wt%). Wm tuffs

TABLE 2. COMPOSITION OF GLASS SHARDS—ELECTRON PROBE MICROANALYSES

Age (Ma)	Type*	Ash bed	Sample number	n†	SiO2§ [.5]	TiO2 [.01]	Al2O3 [.2]	Fe2O3# [.03]	MnO [.005]	MgO [.01]	CaO [.02]	BaO [.02]	Na2O [.2]	K2O [0.3]	Cl [.004]	F [.03]	H2O** [1.0]	–O [.03]	Total [1.0]
6.00	Gm	Wolverine Creek	acb92-6a	18	72.8	0.12	11.6	1.30	0.035	0.07	0.48	0.03	2.9	5.5	0.125	0.12	5.9	0.08	100.9
7.02	Gm	Cub River	rv88- 2	23	73.5	0.19	11.4	1.13	0.030	0.08	0.44	0.03	2.7	5.6	0.100	0.23	5.5	0.12	100.8
7.05	Gm	Rattlesnake	clk93-08	15	72.7	0.11	11.4	1.02	0.090	0.03	0.25	0.03	2.4	6.6	0.080	0.07	5.3	0.05	100.0
7.49	Gm	Faust	rv88-15a	26	73.1	0.19	11.3	1.29	0.025	0.08	0.44	0.03	2.5	6.0	0.077	0.21	4.7	0.10	99.8
7.62	Gp	Shoofly Creek	poc94-556	20	73.6	0.11	10.8	2.10	0.040	0.01	0.16	0.00	2.7	6.2	0.109	0.16	4.8	0.09	100.6
7.90	Gm	Rush Valley	rv88-12a	20	72.9	0.18	11.2	1.82	0.035	0.04	0.51	0.04	2.3	5.7	0.025	0.16	5.4	0.07	100.2
8.00	D	Alamo	vvy93-05	15	68.8	0.42	13.1	1.90	0.090	0.28	0.74	0.12	3.7	5.1	0.170	0.11	6.1	0.08	100.6
8.30	Gm	Inkom	rv89-11	20	73.6	0.32	11.3	1.73	0.025	0.13	0.60	0.07	2.3	5.8	0.039	0.20	4.8	0.09	100.8
9.24	Gm	Mink Creek	rv88-10	18	71.7	0.34	11.2	2.17	0.040	0.14	0.78	0.13	2.5	5.5	0.040	0.00	4.7	0.01	99.2
9.46	Wm	Sheep Dip	i88- 69	17	73.4	0.09	12.0	0.77	0.045	0.06	0.49	0.03	2.8	5.5	0.073	0.05	4.7	0.04	100.0
9.52	Gm	Opal Canyon 6	epb92-77	25	72.6	0.27	11.4	2.05	0.035	0.10	0.71	0.11	1.5	6.4	0.040	0.21	5.0	0.10	100.3
9.70	Gm	Section 26	tc90-22	21	71.0	0.34	11.5	2.29	0.040	0.17	0.88	0.07	2.7	5.2	0.030	0.06	5.3	0.03	99.5
9.73	Wm	Celatron	epb92-79	19	71.9	0.16	11.8	1.23	0.035	0.09	0.66	0.08	2.0	6.6	0.089	0.12	4.8	0.07	99.5
9.73	Wm	Quarry G 9	qg-9	18	72.1	0.14	11.9	1.18	0.030	0.09	0.65	0.04	2.2	6.3	0.083	0.09	5.9	0.06	100.7
9.81	Gm	Hazen	qe-6	40	71.7	0.31	11.3	2.26	0.030	0.11	0.76	0.13	2.0	5.9	0.020	0.08	5.9	0.04	100.5
10.19	Gm	Opal Canyon 3	epb92-22	18	71.9	0.29	11.4	2.28	0.040	0.09	0.74	0.09	1.7	6.0	0.023	0.08	5.6	0.04	100.2
10.45	Gm	CPT XV	i88- 61	19	71.2	0.30	11.0	2.54	0.035	0.08	0.72	0.08	2.3	5.8	0.022	0.19	6.0	0.08	100.2
10.54	Gm	Opal Canyon 2	epb92-23	17	72.3	0.28	11.3	2.47	0.025	0.06	0.69	0.08	2.3	4.9	0.026	0.10	6.9	0.05	101.3
11.51	Wm	Coal Valley	i88- 54a	17	73.2	0.08	12.0	0.53	0.060	0.07	0.44	0.13	2.1	6.1	0.073	0.02	5.7	0.03	100.5
11.57	Wm	Ammonia Tanks	sv93-282	21	72.1	0.11	11.5	0.71	0.080	0.04	0.29	0.01	2.5	6.7	0.094	0.20	6.2	0.11	100.5
11.66	Wm	Browns Hill 3	i88- 48	17	73.5	0.14	11.9	0.83	0.050	0.12	0.55	0.11	2.8	5.2	0.167	0.01	5.1	0.04	100.4
11.72	Wm	Rainier Mesa	i88- 47	17	73.0	0.08	11.8	0.57	0.055	0.06	0.35	0.00	2.2	6.6	0.074	0.10	5.9	0.06	100.7
11.79	Wm	Overnight	wb93-320	21	73.6	0.07	11.9	0.53	0.075	0.04	0.32	0.02	2.8	5.5	0.075	0.17	4.2	0.09	99.2
11.82	Gm	Logan Ranch	i90- 8	20	70.8	0.35	11.5	2.24	0.035	0.14	0.82	0.05	2.2	6.3	0.025	0.12	6.0	0.06	100.4
12.01	Wm	Aldrich Hill 2	i88- 88	41	72.6	0.13	11.8	0.82	0.065	0.07	0.44	0.01	2.2	6.7	0.168	0.11	4.3	0.08	99.3
12.07	Wm	Aldrich Hill 1	as92-117b	24	72.6	0.10	11.7	0.66	0.060	0.11	0.69	0.13	1.5	6.4	0.084	0.02	5.9	0.03	100.0
12.83	Wm	Tiva Canyon	i88- 37	16	72.1	0.12	11.6	0.89	0.105	0.04	0.25	0.00	2.4	7.2	0.072	0.13	4.6	0.07	99.4
12.84	Wm	Yucca Mtn	i88- 36	19	71.9	0.12	11.6	0.90	0.100	0.05	0.25	0.00	2.3	7.3	0.065	0.16	4.7	0.08	99.3
12.97	Wm	Badlands	i92-178	19	73.1	0.14	12.0	0.93	0.060	0.17	1.01	0.12	2.4	5.3	0.060	0.08	4.7	0.05	100.0
13.25	Gm	Worthington Mine	tc90-30	21	72.5	0.14	11.4	1.46	0.030	0.06	0.50	0.00	1.6	6.2	0.070	0.08	6.0	0.05	100.0
13.73	Gm	Rawhide Ranch	tc90-41	20	72.2	0.16	11.1	1.14	0.025	0.06	0.51	0.01	1.3	7.2	0.066	0.20	5.6	0.10	99.5
13.78	Gp	Grouse Canyon(?)	sv92- 94a	22	70.4	0.21	10.7	3.66	0.165	0.01	0.22	0.01	1.2	4.7	0.123	0.19	7.9	0.11	99.4
13.90	Gm	Roadcut	htc93-447	19	71.0	0.28	11.6	1.90	0.030	0.11	0.65	0.09	2.0	7.0	0.050	0.20	4.8	0.10	99.6
14.93	Gm	Obliterator	suc92-06a	22	72.1	0.17	11.3	1.90	0.030	0.03	0.58	0.02	1.8	5.3	0.070	0.06	6.4	0.04	99.7
15.18	Gm	Virgin Valley 12	vvy93-12	21	71.4	0.23	11.6	1.97	0.030	0.08	0.56	0.07	1.8	6.6	0.040	0.20	6.3	0.09	100.8
15.17	Gm	Paradise Valley	buf94-618	19	72.2	0.27	11.9	2.32	0.035	0.10	0.67	0.04	2.4	6.2	0.040	0.27	4.3	0.12	100.6
15.21	Gm	Huntington Creek 2	buf94-617	19	72.3	0.25	11.8	2.52	0.045	0.09	0.69	0.04	2.5	6.2	0.045	0.22	4.5	0.10	101.1
15.21	Gm	Huntington Creek 1	htc93-439	20	71.3	0.25	11.6	2.38	0.050	0.07	0.66	0.08	2.0	6.9	0.045	0.22	5.3	0.10	100.7
15.24	Gm	Antonne Wash	buf94-616	20	73.0	0.20	11.5	2.35	0.040	0.01	0.63	0.01	2.5	6.1	0.070	0.28	4.6	0.13	101.2
15.41	Gm	Virgin Valley 8	vvy93-8	20	70.9	0.23	11.1	2.70	0.050	0.03	0.65	0.09	1.5	5.9	0.040	0.16	6.7	0.07	99.4
15.50	Gp	Overton Wash	wcr91-13	20	71.8	0.14	10.9	1.91	0.100	0.04	0.15	0.02	1.9	6.7	0.092	0.12	6.2	0.07	100.0
15.54	Gm	Virgin Valley 1	buf94-601	20	69.9	0.35	11.7	4.18	0.095	0.11	1.21	0.12	2.7	4.8	0.024	0.20	5.4	0.09	100.7
16.00	Gp	Peacock	buf94-596	20	72.3	0.25	11.0	2.01	0.110	0.09	0.10	0.00	1.6	6.9	0.113	0.18	6.4	0.10	101.0

*D—dacite; Gm—gray metaluminous rhyolite; Gp—gray peralkaline rhyolite; Wm—white metaluminous rhyolite.
†Number of analyzed glass shards.
§All oxides and elements in wt%. Values in brackets are estimated analytical precision (1σ) for a typical mean analysis of 20 shards.
#Total Fe reported as Fe_2O_3.
**H_2O content calculated from difference between measured and stoichiometric oxygen content assuming all Fe as Fe_2O_3.

TABLE 3. COMPOSITION OF GLASS SHARDS—X-RAY FLUORESCENCE SPECTROMETRY

Age (Ma)	Type*	Ash bed	Sample number	Fe† [.021]	Ca† [.014]	Ba [20]	Mn [5]	Nb [1]	Rb [4]	Sr [2]	Ti [30]	Y [5]	Zn [6]	Zr [8]	La [5]	Nd [5]	Th [2]	Ce [15]
6.00	Gm	Wolverine Creek	acb92- 6A	0.85	0.31	453	211	57	166	15	683	69	72	177	70	60	24	140
7.02	Gm	Cub River	brc92-15	0.72	0.29	233	180	41	206	13	1020	60	25	184	64	48	32	121
7.05	Gm	Rattlesnake	brc92-14	1.13	0.23	985	626	24	71	10	772	54	106	361	45	58	9	110
7.49	Gm	Faust	rv88-15a	0.82	0.29	329	166	41	198	16	1138	61	30	234	76	53	29	140
7.62	Gp	Shoofly Creek	poc94-556	1.27	0.06	12	247	27	118	1	621	99	124	566	42	53	16	110
7.90	Gm	Rush Valley	rv88-12a	1.17	0.34	480	257	56	181	19	1068	76	52	319	84	69	27	167
8.00	D	Alamo	vvy93-05	N.A.§	N.A.	N.A.	N.A.	N.A.	N.A.	N.A.	N.A.	N.A.	N.A.	N.A.	N.A.	N.A.	N.A.	N.A.
8.30	Gm	Inkom	rv89-11	1.10	0.44	895	187	40	177	37	1872	52	29	381	69	51	27	128
9.24	Gm	Mink Creek	rv88-10	1.40	0.55	1004	250	46	158	49	1982	57	41	456	74	61	24	138
9.46	Wm	Sheep Dip	i88- 69	0.49	0.34	373	309	17	137	59	568	19	17	84	37	27	20	68
9.52	Gm	Opal Canyon 6	epb92-77	1.35	0.51	970	212	43	170	42	1546	48	32	389	82	62	26	160
9.70	Gm	Section 26	tc90-22	1.44	0.56	971	276	45	160	52	2002	55	39	482	71	60	24	134
9.73	Wm	Celatron	qg-11	0.78	0.54	542	220	30	146	60	897	45	30	175	75	57	20	142
9.73	Wm	Quarry G 9 ash	qg- 9	0.72	0.46	566	200	28	146	45	820	43	27	143	74	57	21	144
9.81	Gm	Hazen	qe- 6	1.43	0.51	1066	216	40	180	44	1804	59	40	445	74	54	26	140
10.19	Gm	Opal Canyon 3	epb92-22	1.57	0.59	1114	232	40	168	48	1785	60	46	449	66	57	26	146
10.45	Gm	CPT XV	i88- 61	1.56	0.47	1008	233	45	179	35	1592	64	52	475	81	65	26	160
10.54	Gm	Opal Canyon 2	epb92-23	1.65	0.56	1098	257	46	168	50	1635	71	60	449	73	64	26	162
11.51	Wm	Coal Valley	i88- 54a	0.33	0.33	1132	419	10	98	77	522	8	22	43	12	16	11	30
11.57	Wm	Ammonia Tanks	i88- 52a	0.49	0.21	92	525	33	190	16	809	42	65	138	35	30	25	63
11.66	Wm	Browns Hill 3	i88- 48	0.55	0.39	1074	372	7	110	73	887	13	24	101	27	24	13	45
11.72	Wm	Rainier Mesa	i88- 47	0.41	0.25	22	360	24	202	10	689	35	28	87	33	28	24	69
11.79	Wm	Overnight ash	wb93-320	N.A.	N.A.	N.A.	N.A.	N.A.	N.A.	N.A.	N.A.	N.A.	N.A.	N.A.	N.A.	N.A.	N.A.	N.A.
11.82	Gm	Logan Ranch	i90- 8	1.46	0.57	954	242	38	178	49	2015	55	36	450	71	57	25	144
12.01	Wm	Aldrich Hill 2	i88- 88	0.51	0.27	140	465	22	248	33	778	43	31	112	40	33	41	77
12.07	Wm	Aldrich Hill 1	as93-117b	N.A.	N.A.	N.A.	N.A.	N.A.	N.A.	N.A.	N.A.	N.A.	N.A.	N.A.	N.A.	N.A.	N.A.	N.A.
12.83	Wm	Tiva Canyon	i88- 37	0.55	0.16	56	715	25	172	11	754	38	63	186	31	31	22	65
12.84	Wm	Yucca Mountain	i88- 36	0.54	0.13	7	715	26	196	8	734	43	66	173	31	31	23	59
12.97	Wm	Badlands	sv92-91a	N.A.	N.A.	N.A.	N.A.	N.A.	N.A.	N.A.	N.A.	N.A.	N.A.	N.A.	N.A.	N.A.	N.A.	N.A.
13.25	Gm	Worthington Mine	wb93-311	0.89	0.33	59	146	49	262	11	833	50	43	203	83	59	33	176
13.73	Gm	Rawhide Ranch	tc90-41	0.84	0.33	137	125	39	250	12	884	75	31	199	82	55	37	163
13.78	Gp	Grouse Canyon?	sv92- 94a	2.38	0.12	<1	1213	58	161	1	1196	81	162	933	137	101	23	267
13.90	Gm	Roadcut	htc93-447	1.15	0.42	727	160	27	172	33	1496	51	28	468	64	44	22	121
14.93	Gm	Obliterator	suc92-06a	1.23	0.39	128	216	36	169	7	1008	48	48	308	82	69	28	150
15.18	Gm	Virgin Valley 12	vvy93-12	1.41	0.44	728	241	38	172	25	1557	75	45	446	75	62	24	146
15.17	Gm	Paradise Valley	buf94-618	1.57	0.46	826	299	40	164	27	1459	80	62	473	77	66	21	135
15.21	Gm	Huntington Creek 2	buf94-617	1.46	0.42	671	282	41	166	24	1362	72	60	423	73	63	23	147
15.21	Gm	Huntington Creek 1	htc93-439	1.80	0.47	845	394	45	153	24	1421	98	98	568	80	77	17	152
15.24	Gm	Antonne Wash	buf94-616	1.46	0.43	380	258	41	153	11	1131	99	131	440	95	81	20	181
15.41	Gm	Virgin Valley 8	vvy93-08	1.78	0.48	802	420	43	183	23	1402	62	91	559	91	73	21	172
15.50	Gp	Overton Wash	wcr91-13	1.22	0.09	1	755	25	231	4	854	74	82	511	58	57	21	124
15.54	Gm	Virgin Valley 1	buf94-601	2.59	0.84	1396	651	28	121	88	2032	72	88	465	58	52	17	135
16.00	Gp	Peacock	buf94-596	1.29	0.03	13	811	28	211	1	1418	79	102	589	43	57	23	111

*D = dacite; Gm = gray metaluminous rhyolite; Gp = gray peralkaline rhyolite; Wm = white metaluminous rhyolite.
†Fe and Ca in wt% and all other elements in ppmw; values in brackets are estimated precision of analyses (1σ).
§N.A. = not analyzed.

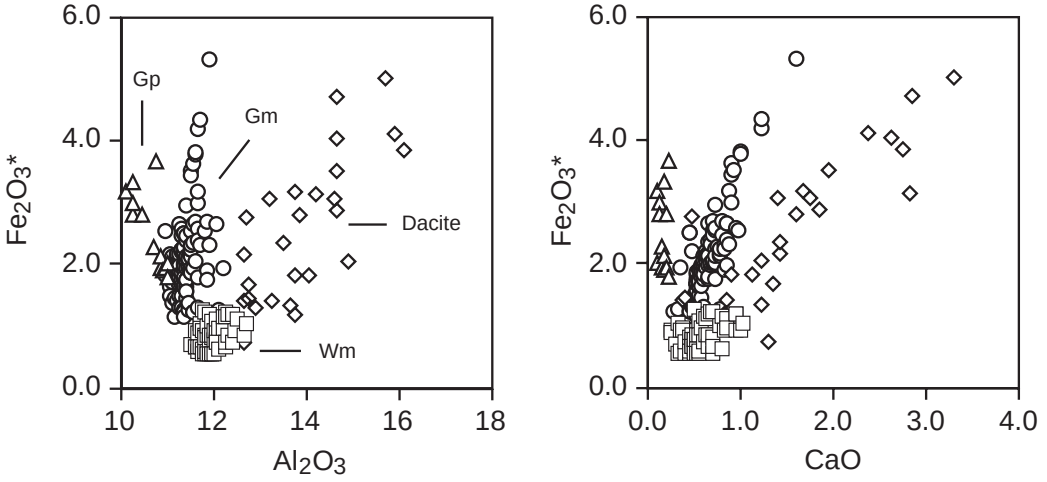

Figure 2. Major glass shard compositional groups. Fe_2O_3* (total Fe as Fe_2O_3), Al_2O_3, and CaO content in glass shards. Electron probe analyses with contents in wt%. Analyses for the 213 different ash beds identified in the sampled sections. Each data point is an average of ~20 individual shard analyses. Gm—gray metaluminous rhyolite glass (circles); Gp—gray peralkaline rhyolite glass (triangles); Wm—white metaluminous rhyolite glass (squares); Dacite—dacite glass (diamonds).

are within the field of Izett's W-type (white-type) rhyolitic glasses, and our dacite tuffs are within Izett's field of dacitic glasses.

CORRELATION OF TUFFS

Of the 213 tuff beds identified in this study, 59 are correlated between the principal and/or ancillary sections and/or to named ash-flow tuffs within a source area. We refer to these 59 tuff beds as the correlative tuffs or ash beds. The distributions of the correlative tuffs, which link the principal and ancillary sections and establish a composite sequence of vitric tuffs for basins, are shown in Figure 3. All of the correlative tuffs have been named. Ash beds correlated to named ash-flow tuffs are given the name of the ash-flow tuff. Otherwise, whenever feasible, we use geographic place names for tuffs.

Our basic approach to correlation is that of Sarna-Wojcicki and Davis (1991), which is, in essence, to correlate by glass composition but to confirm with sequence (i.e., the position of the ash bed relative to other ash beds). The correlation of the CPT IX ash bed, discussed below, gives an example of correlation on the basis of glass composition with correlation confirmed by sequence. Most of our correlations are of this type. For some ash beds this approach is modified in that both composition and sequence are used in concert to establish correlation. This approach is used for the ~10% of the samples in Figure 3 for which only electron probe analyses are available. Such analyses may not uniquely characterize an ash bed. It is also the approach used for those few ash beds that are not uniquely characterized by XRF analyses of glass shards. The example we give of the correlation of four Wm ash beds to specific ash-flow tuffs in the southwestern Nevada volcanic field illustrates correlation by composition and sequence.

Examples

CPT IX Ash Bed. The CPT IX ash bed is a ca. 11.6 Ma Gm ash bed identified throughout the northern Basin and Range (Fig. 3). The CPT IX ash bed is named after unit IX of the Cougar Point Tuff, one of nine welded ash-flow tuff units recognized by Bonnichsen (1982) in the Bruneau-Jarbidge volcanic field of the Snake River Plain volcanic province. Although the CPT IX ash bed, like many Gm ash beds, has a glass shard composition quite similar to several other Gm ash beds, it can confidently be differentiated from such ash beds on the basis XRF analyses alone.

The "uniqueness" of XRF analyses of glass shard separates from the CPT IX ash bed is illustrated in Table 4. This table includes typical analyses of CPT IX ash-bed samples from throughout the northern Basin and Range, including sample brv93–430 from basal fallout tuff of unit IX of the Cougar Point Tuff. For comparison, Table 4 also includes analyses of other ash beds that are most similar in composition to the CPT IX ash bed. Also given in Table 4 are the values for the statistical distance, *D*, the statistic used in this study to assess similarities and differences between analyses. This statistic, discussed fully by Perkins et al. (1995b), is the normalized Euclidean distance between analyses with estimated analytical precision used to normalize the analyses (see Table 4 notes for formula). The *D* values in Table 4 compare the average of 12 CPT IX analyses in our database with the analyses in the table. Here *D* is calculated for the five elements that best differentiate this particular group of ash beds: Ba, Mn, Rb, Ti, and Zr. For analyses statistically identical to the CPT IX average we expect $D \leq 3.9$ ($D^2 \leq 15.1$) at the 99% confidence level. This is what we find for the six CPT IX samples in Table 4. Equally important, all other samples in Table 4 have $D \geq 5.3$, and, thus, are statistically distinct from the CPT IX samples. Thus we conclude that samples grouped as the CPT IX ash bed, including the type CPT IX sample, brv93–430, have statistically identical compositions and are compositionally distinct from other ash beds of similar composition. Inspection of Figure 3 confirms that the samples identified as the CPT IX ash bed in Table 4 are in proper stratigraphic sequence with respect to other correlative ash beds. Compositionally unique ash beds such as the CPT IX ash bed are the foundation for establishing the composite sequence of northern Basin and Range tuffs.

Southwestern Nevada Volcanic Field Ash Beds. We correlate four Wm ash beds with ash-flow tuffs in the southwestern Nevada volcanic field: the Ammonia Tanks Tuff, the Rainier Mesa Tuff, the Tiva Canyon Tuff, and the Yucca Mountain Tuff. Some electron probe analyses of pumices have been reported for these tuffs, and we use these analyses along with sequence and age to correlate between these ash-flow tuffs and northern Basin and Range ash beds.

The essence of the correlation of Wm ash beds to southwestern Nevada volcanic field ash-flow tuffs is in Table 5. Table 5 is a distance matrix that shows the statistical distance between electron probe analyses of glass shards from Wm ash beds and pumice glasses from southwestern Nevada volcanic field ash-flow tuffs. The Wm ash beds are those of the Ibapah Badlands, the section with one of the best records of Wm ash beds (26 Wm ash beds). The pumice analyses, reported by Warren et al. (1989), are from the four largest metaluminous ash-flow tuff sheets in the southwestern Nevada volcanic field: the 11.57 (11.45) Ma Ammonia Tanks Tuff; the 11.72 (11.60) Ma Rainier Mesa Tuff; the 12.83 (12.70) Ma Tiva Canyon Tuff; and the 12.93 (12.80) Ma Topopah Spring Tuff (Sawyer et al., 1994). Our evaluation of the analyses of Warren et al. (1989) indicates that their data set contains 13 compositionally distinct pumice glasses. The Table 5 distance matrix is a subset of the full matrix with only those pumice-type ash-bed pairs with $D \leq 6$. In the combined compositional sequence comparison, a sequence of candidate correlations clearly emerges. These are the underlined entries in the Table 5. The sequence is not completely unique because there are some competing pairs of potential correlations. These conflicts are resolved with additional considerations.

For i88-52a there is only one good composition and age match, and that is AT-Uii, one of the pumice types from the upper part of the Ammonia Tanks Tuff. For the i88-47/49 pair we note that only the i88-47 ash bed is widely distributed (Fig. 3). The i88-49 ash bed, which is 8 m above the i88-47 ash bed, is identified only in the Ibapah Badlands section. We conclude that the i88-47 ash bed is the ash bed associated with the eruption of the large volume Rainier Mesa Tuff. A $^{40}Ar/^{39}Ar$ date of 11.74 ± 0.03 Ma on a correlative of the i88-47 ash bed in Stewart Valley (Fig. 3) strongly supports correlation of the i88-47 to the 11.72 (11.60) Ma Rainier Mesa Tuff. For the i88-36/37 pair we correlate the upper ash bed, i88-37, with the Tiva Canyon Tuff and the lower (by 1 m) ash bed with the slightly older Yucca Mountain Tuff. Warren et al. (1989) did not analyze pumices from the Yucca Mountain Tuff, but whole rock trace element analyses of Flood et al. (1989) indicate that high silica rhyolite components of both the Tiva Canyon Tuff and Yucca Mountain Tuff are similar. Thus, we conclude that the compositionally similar i88-36/37 pair (Table 3) correlates to this pair of ash-flow tuffs. Sample i88-29b is a potential compositional match to Topopah Springs pumice, but appears to be too old to be the Topopah Springs ash bed. We conclude that the Topopah Spring ash bed may not be present in the Ibapah Badlands section, or if it is present, it has a glass composition different than the reported analyses of pumices from the Topopah Spring Tuff.

AGE OF TUFFS

We estimated ages of all correlative tuffs. These ages are listed in the "Age" columns on the sides of the correlation chart (Fig. 3). These ages include isotopic dates and interpolation (more rarely, extrapolation) age estimates. The 22 isotopic dates, highlighted in bold in the "Age" columns, are control dates. The interpolation and extrapolation age estimates, discussed below, are calculated ages relative to the control dates. The control dates are a set of 18 high-precision and four moderate-precision isotopic

Ash Bed/Horizon	Type	Age (Ma)	sd (Ma)
Wolverine Creek ash	Gm	6.00	0.20
Walcott ash	Gm	**6.40**	**0.10**
Blacktail Creek ash	Gm	**6.70**	**0.10**
Cub River ash	Gm	7.02	0.10
Rattlesnake ash	Gm	**7.05**	**0.01**
Faust ash	Gm	**7.49**	**0.04**
Shoofly Creek ash	Gp	7.62	0.10
Rush Valley ash	Gm	7.90	0.50
Alamo ash	D	8.00	1.00
Inkom ash	Gm	8.30	0.50
ash bed	D	**8.50**	**0.13**
ash-flow tuff	Gm	**8.84**	**0.04**
Mink Creek ash	Gm	9.24	0.50
ash bed	Gm	9.36	0.20
Sheep Dip ash	Wm	9.46	0.20
Opal Canyon 6 ash	Gm	9.52	0.20
Section 26 ash	Gm	9.70	0.20
Celatron ash	Wm	9.73	0.20
Quarry G 9 ash	Wm	9.73	0.20
ash bed	D	**9.79**	**0.13**
Hazen ash	Gm	9.81	0.20
ash-flow tuff	Gm	**10.13**	**0.03**
Opal Canyon 3 ash	Gm	10.19	0.10
CPT XV ash	Gm	10.45	0.10
Opal Canyon 2 ash	Gm	10.54	0.16
Ibex Peak 19 ash	Gm	10.74	0.10
CPT XIII ash	Gm	**10.94**	**0.03**
lava flow	– – –	11.10	0.10
CPT XII ash	Gm	11.19	0.10
CPT XI ash	Gm	11.31	0.10
Coal Valley ash	Wm	11.51	0.10
Ammonia Tanks ash	Wm	**11.57**	**0.05**
CPT IX ash	Gm	11.59	0.10
Browns Hill ash	Wm	11.66	0.10
Rainier Mesa ash	Wm	**11.72**	**0.05**
Overnight ash bed	Wm	11.78	0.10
Logan Ranch ash	Gm	11.82	0.10
Ibex Peak 8 ash	Gm	11.80	0.04
Ibex Hollow ash	Gm	**11.93**	**0.03**
Aldrich Hill 2 ash	Wm	12.01	0.10
Aldrich Hill 1 ash	Wm	12.07	0.10
White Basin ash	Gm	12.02	0.10
CPT V ash	Gm	**12.07**	**0.04**
Banded ash	Gm	12.14	0.10
Pictograph ash	Gm	12.34	0.10
CPT III ash	Gm	**12.67**	**0.03**
Tiva Canyon ash	Wm	**12.83**	**0.05**
Yucca Mountain ash	Wm	12.84	0.06
Grant claim ash	Gm	**12.96**	**0.04**
Badlands ash	Wm	12.97	0.10
Worthington Mine ash	Gm	13.25	0.50
Rawhide Ranch ash	Gm	13.73	0.16
Grouse Canyon? ash	Gp	**13.78**	**0.04**
ash bed	Gm	**13.89**	**0.04**
Roadcut ash	Gm	13.90	0.25
Obliterator ash	Gm	**14.93**	**0.08**
Virgin Valley 12	Gm	15.18	0.03
Paradise Valley ash	Gm	**15.17**	**0.05**
Huntington Creek 2 ash	Gm	15.21	0.25
Huntington Creek 1 ash	Gm	15.21	0.25
Antonne Wash ash	Gm	15.24	0.25
Virgin Valley 8 ash	Gm	15.41	0.25
"Gilbert Andesite"	– – –	15.50	0.25
Overton Wash ash	Gp	15.50	0.25
Virgin Valley 1 ash	Gm	15.54	0.25
ash bed	Wm	**15.84**	**0.05**
Peacock ash	Gp	16.00	0.25
ash bed	D	16.05	0.25
Canyon Rhyolite	– – –	16.28	0.02

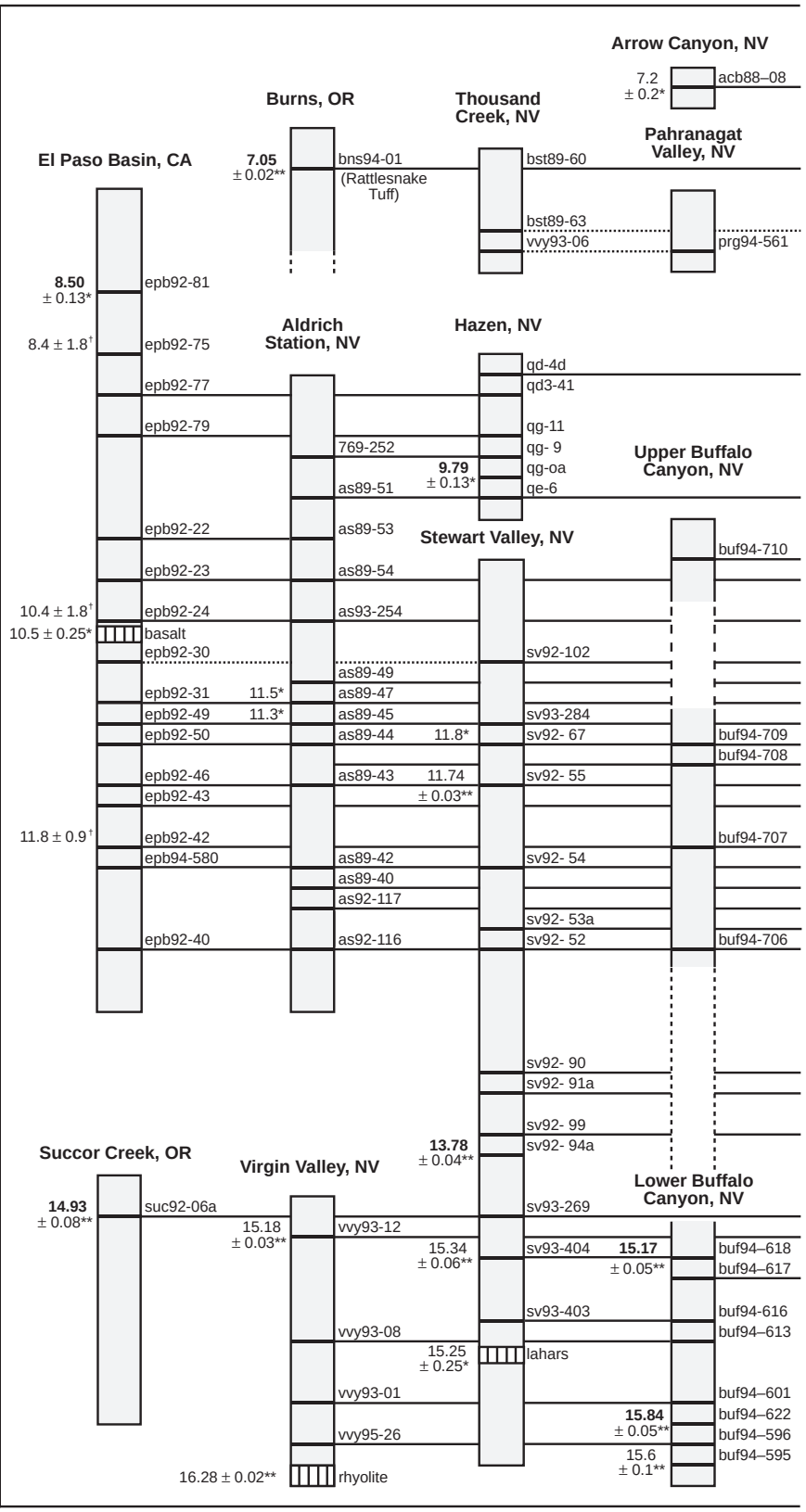

Figure 3. Correlation chart. Tie lines link correlative ash beds (dashed tie lines indicate more speculative correlations). Name of correlative ash bed or other units is given in the leftmost column—ash beds with underlined names are named after correlative ash-flow tuff units. Ash bed group is given in the next column: D—dacite; Gp—gray peralkaline rhyolite; Gm—gray metaluminous rhyolite; Wm—white metaluminous rhyolite. Age and error estimates of ash beds and other horizons are given in following two columns. Ages in boldface type are the isotopic age estimates

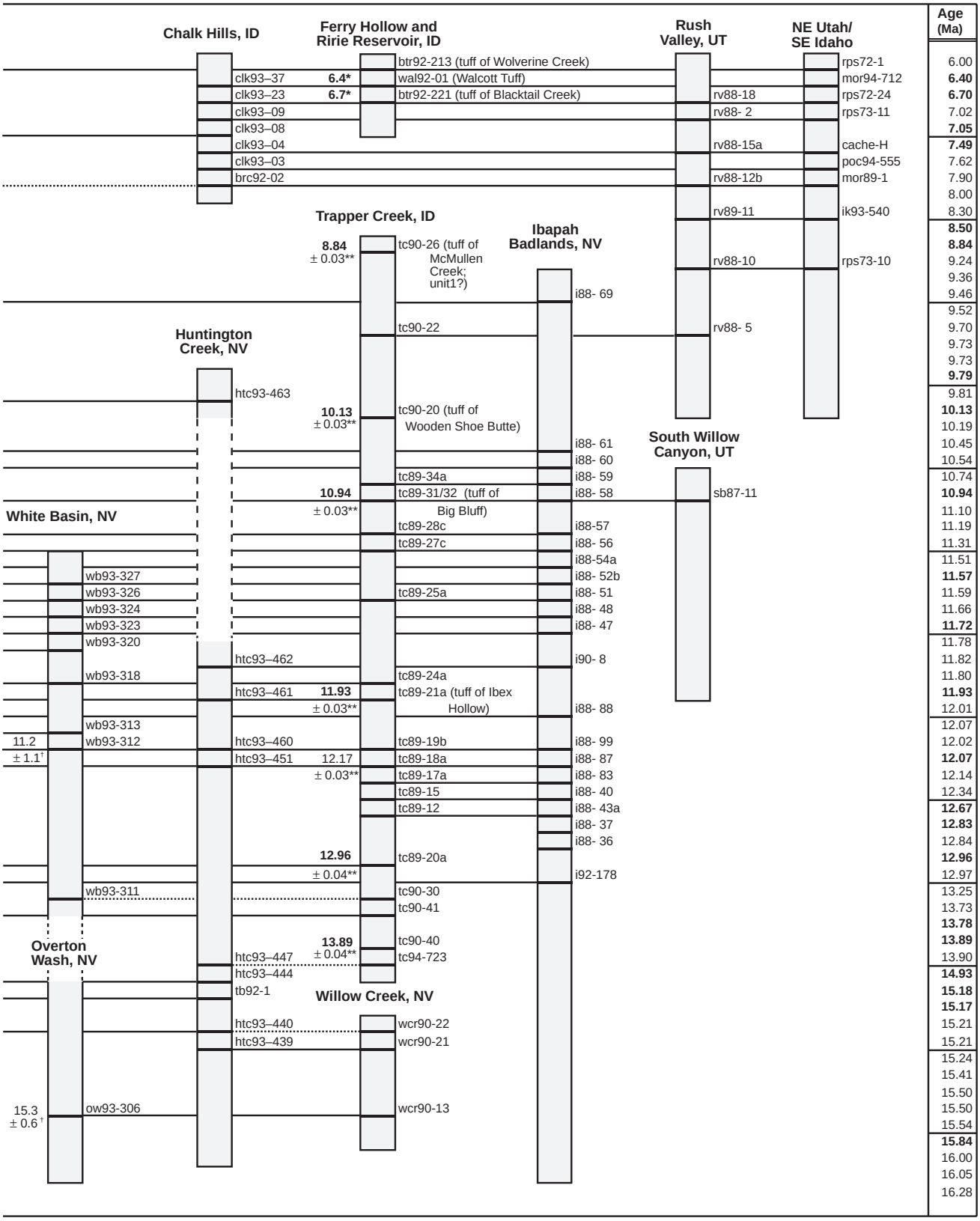

used for primary age control; most other ages in "Age" column are interpolation or extrapolation age estimates. Ash-bed sample numbers are listed on the right side of the sections. Isotopic ages reported for horizons in an individual section are given along left side of section. Isotopic ages include $^{40}Ar/^{39}Ar$ ages flagged by "", K-Ar ages flagged by "*", and fission-track zircon ages flagged by "†". Time intervals in sections highlighted by dashed lines are missing (upper Buffalo Canyon), excised by fault (Huntington Creek), or not sampled.**

TABLE 4. GLASS COMPOSITION (X-RF) OF THE CPT IX ASH BED AND SEVERAL SIMILAR ASH BEDS

Sample	Ash bed	Fe*	Ca	Ba	Mn	Rb	Sr	Ti	Zr	D†
as92-116	CPT V	1.13	0.37	513	187	199	26	1045	285	11.5
i88-103	CPT V	1.15	0.38	554	193	198	29	1091	295	10.2
brv93-427	CPT V	1.15	0.37	542	191	197	27	1084	298	10.0
htc93-449	CPT V	1.15	0.36	485	189	208	25	1075	303	10.0
tc89-18a	CPT V	1.15	0.39	545	191	201	27	1235	299	6.6
sv92-52	CPT V	1.22	0.40	591	194	194	32	1152	295	9.4
as89-44	CPT IX	1.13	0.36	520	166	200	24	1303	320	3.2
brv93-430	CPT IX	1.14	0.35	540	165	199	22	1310	340	2.5
tc89-25a	CPT IX	1.14	0.37	584	176	199	25	1342	338	2.9
i88-51	CPT IX	1.17	0.38	496	176	208	24	1347	349	2.0
sv92-67	CPT IX	1.17	0.39	513	172	201	24	1332	340	1.2
epb92-50	CPT IX	1.19	0.39	550	183	217	26	1398	336	3.8
i88-79	Unnamed	1.19	0.37	609	192	197	29	1328	348	5.3
dch91-05	Unnamed	1.20	0.39	534	167	230	30	1575	332	9.3
mon91-06	Unnamed	1.21	0.39	537	159	225	25	1550	341	8.4

*Element concentrations and analytical precisions as in Table 2.

†Statistical distance from average of CPT IX analyses using Ba, Mn, Rb, Ti, and Zr. These five elements best differentiate the CPT IX glass from glass of compositionally similar tuffs. Distance formula is

$$D^2 = \sum_{k=1}^{n} \left(x_{k1} - x_{k2}\right)^2 \Big/ \left(\sigma_{k1}^2 + \sigma_{k2}^2\right)$$

where n is the number of elements in comparison, x_{k1} and x_{k2} are concentration of k^{th} element in 1st and 2nd sample, respectively, and σ_{k1} and σ_{k1} are the respective standard deviations of precision for the measured concentrations of the k^{th} element. When two analyses with the same precision are compared, $\sigma_{k1} = \sigma_{k2} = \sigma_k$. When x_{k2} is the mean of m analyses, as in this table $\sigma_{k2} = \sigma_{k1}/\sqrt{m}$; m = 12, the number of analyses used for mean of CPT XI ash bed. D^2 has a Chi-square distribution among compositionally identical samples (Perkins et al., 1995b). Thus for a five element comparison of identical samples, D = 3.3 (D^2 = 11.1) at 95% confidence level, and D = 3.9 (D^2 = 15.1) at 99% confidence level.

TABLE 5. DISTANCE MATRIX COMPARING SWNVF PUMICES AND IBAPAH BADLANDS WM RHYOLITE TUFFS

	Pumices [Age]						
Ash bed [Age]	TS–N [12.93]	TC–Uia [12.83]	TC–N [12.83]	RM–L [11.72]	RM–U [11.72]	AT–L [11.57]	AT–Uii [11.57]
i92-211 [8.98]	9	5	8	11	9	9	5
i92-209 [8.99]	9	5	7	11	9	8	5
i88-69 [9.46]	2.8	10	11	8	7	8	10
i88-52a [11.53]	7	3.9	4	8	5	4	3.5*
i88-49 [11.58]	5	7	7	6	3.3	4	5
i88-47 [11.74]	8	8	8	4	3.1*	5	6
i88-88 [12.01]	5	8	8	9	6	6	7
i88-36 [12.91]	10	3.2*	3.9	12	9	7	5
i88-37 [12.92]	10	3.2*	3.9	12	9	7	4
i88-31 [13.07]	7	6	8	11	9	8	7
i88-30 [13.09]	6	6	8	10	8	8	7
i88-29b [13.31]	3.5	9	11	8	7	8	9

Note: Stratigraphic sequence of Ibapah Badlands samples is youngest at top to oldest at base. Stratigraphic sequence of southwest Nevada volcanic field (SWNVF) pumices is oldest at left to youngest at right. TS—pumice samples from Topopah Spring Tuff; TC—pumice samples from Tiva Canyon Tuff; RM—pumice samples from Rainier Mesa Tuff; AT—pumice samples from Ammonia Tanks Tuff. Electron probe analyses of Fe, Ti, Mn, Mg, Ca, and Ba are compared in this matrix. Assumed standard deviations (σk) for concentrations are: Fe—0.03; Ca—0.02; Ti, Mn, Mg, Ba—0.01 and the distance formula is

$$D^2 = \sum_{k=1}^{n} \left(x_{k1} - x_{k2}\right)^2 \Big/ 2\sigma_k^2$$

Formula parameters are described in Table 5. Distances <3.95 are given to one decimal place. Underlined distances identify sample pairs that are potential correlatives based on composition, estimated age, and sequence. Distances with asterisks identify correlated sample pairs discussed in text.

dates spanning the age range of the northern Basin and Range sections. The high-precision dates include $^{40}Ar/^{39}Ar$ laser-fusion dates from seven horizons dated in this study (Table 6) and another 11 $^{40}Ar/^{39}Ar$ laser-fusion dates reported in other studies (Table 7). The moderate precision dates are K-Ar dates (Table 7). These dates are used in intervals that lack high-precision $^{40}Ar/^{39}Ar$ dates.

An additional 20 isotopic dates, termed supplementary isotopic dates, have also been reported for tuffs and lavas in the northern Basin and Range sections. These dates are shown in Figure 3 along the left side of the appropriate stratigraphic column and are described in Table 8. The supplementary dates are either of lower precision than the selected control dates, are of suspect accuracy, or are redundant (i.e., they statistically have the same age and precision as a selected control date). They are excluded as control dates for these reasons, but it is important to note that most supplemental isotopic dates are compatible with our estimated dates (Fig. 3). Other supplementary dates are the magnetochronologic dates reported for the El Paso basin section (Burbank and Whistler, 1987; Whistler and Burbank, 1992). There is good concordance between magnetochronology and our age estimates in the upper part of the El Paso basin section (above the basalt, Fig. 3), so these magnetochronologic dates are essentially "redundant" for this time interval. Lower in the section there is a discordance of up to ~0.9 m.y. between the magnetochronology and our age estimates. Until this discordance is resolved we prefer to use isotopic control dates in this time interval.

Interpolation or extrapolation age estimates are calculated relative to two reference horizons. These horizons are either control horizons, horizons for which interpolation age estimates are available from another section (and referenced to control dates), or a combination of these two types of horizons. Constant sediment accumulation rates are assumed for the interval containing the reference horizons and the "unknown" horizon. A linear model, although clearly an approximation, appears to be appropriate for most sections. For example, in a number of the sections there is a strikingly linear rate of sediment accumulation throughout the section (Fig. 4), whereas in other sections, such as the Trapper Creek section (Perkins et al., 1995b), average rates of sediment accumulation vary but are reasonably linear over intervals of ≤1 m.y. In the sections we use for interpolation age estimates the reference horizons are mostly spaced at intervals of ≤1 m.y.

Several observations indicate that interpolation and extrapolation age estimates provide both unbiased and relatively precise age estimates. As seen in Table 9 and discussed earlier, the interpo-

TABLE 6. SUMMARY OF NEW Ar^{40}/Ar^{39} LASER-FUSION DATES

Sample*	Ash bed/unit	n†	K/Ca§	SE#	Age§ (Ma)	SE#	SE w/J**	Comments
tw94-672	Faust	24	9.4	1.7	7.493	.032	.037	Fallout tuff. Multigrain analyses. 14 small and 1 older sanidine groups deleted.
tc90-26	Tuff of McMullen	18	13.4	0.3	8.840	.018	.029	Base surge tuff. Lower K/Ca sanidines.
tc90-26	Creek (unit 1?)	18	21.6	1.4	9.164	.020	.030	Base surge tuff. Higher K/Ca sanidines.
wjr93-436	CPT V	14	16.3	1.1	12.071	.021	.037	Fallout tuff. 5 plagioclases deleted.
tc89-18a	CPT V	14	17.5	1.1	12.169	.011	.032	Fallout tuff. 1 older sanidine deleted.
CPT III	CPT III	63	27.1	0.9	12.669	.010	.033	Basal vitrophyre of ash-flow tuff. 2 younger and 3 older sanidines deleted.
sv92-94a	Grouse Canyon(?)	14	20.9	5.8	13.783	.012	.036	Fallout tuff.
sv93-404	Paradise Valley	10	10.3	0.9	15.342	.050	.063	Fallout tuff. Multigrain analyses.
buf94-618	Paradise Valley	12	9.0	1.0	15.170	.032	.050	Fallout tuff. Multigrain analyses. 2 older sanidine groups deleted.
buf94-622	Unnamed	37	35.1	5.2	15.836	.024	.046	Fallout tuff. Multigrain analyses. 35 small and 2 older sanidine groups deleted.

*Sample locations given in Appendix A.
†Number of analyses.
§Mean K/Ca or age, but see comments. Note slight to moderate discordance in dates of three units. For these three units the younger date is our preferred date on the assumption that the older date reflects minor contamination by older sanidine. Ages relative to Fish Canyon sanidine (27.84 Ma).
#Standard error of the mean.
**SE w/J is standard error of the mean including average error for J of ± 0.25%. SE w/J = $\sqrt{\left(SE^2 + 0.0025^{2*}t^2\right)}$

TABLE 7. ADDITIONAL CONTROL HORIZON DATES

Fallout ash bed	Correlative ash-flow tuff	Age (Ma)*	Reported Age (Ma)†	Analytical Technique§	Rock Type#	Dated Material**	Data sources/comments
Walcott	Walcott Tuff	6.4 ± 0.1		K-Ar	af	wr	Average of four dates listed in Morgan (1992)
Blacktail Creek	Tuff of Blacktail Creek	6.7 ± 0.1		K-Ar	af	fsp	Average of the three dates listed in Morgan (1992)
Rattlesnake	Rattlesnake Tuff	7.05 ± 0.01		LF(s)	af	san	Streck and Grunder (1995)
Unnamed	Unknown	8.50 ± 0.13		K-Ar	f	nr	Whistler and Burbank (1992)
Unnamed	Unknown	9.79 ± 0.13		K-Ar	f	bi/pl	Average of two concordant dates in Brown (1986)
Not identified	Tuff of Wooden Shoe Butte	10.13 ± 0.03	10.02	LF(m)	af	san	Perkins et al. (1995b)
CPT XIII ash	Cougar Point Tuff unit XIII	10.94 ± 0.03		LF(m)	af	san	Perkins et al. (1995b)
Ammonia Tanks	Ammonia Tanks Tuff	11.57 ± 0.05	11.45	LF(s)	af	san	Sawyer et al. (1994)
Rainier Mesa	Rainier Mesa Tuff	11.72 ± 0.05	11.60	LF(s)	af	san	Sawyer et al. (1994)
Ibex Hollow	Tuff of Ibex Hollow	11.93 ± 0.03	11.81	LF(m)	af	san	Perkins et al. (1995b)
Tiva Canyon	Tiva Canyon Tuff	12.83 ± 0.05	12.70	LF(s)	af	san	Sawyer et al. (1994)
Grant Claim	Unknown	12.96 ± 0.04	12.82	LF(m)	f	san	Perkins et al. (1995b)
Unnamed	Unknown	13.89 ± 0.04	13.74	LF(m)	f	san	Perkins et al. (1995b)
Obliterator	Unknown	14.93 ± 0.08		LF(s)	f	fsp	Downing and Swisher (1993)
Virgin Valley 12	Unknown	15.18 ± 0.03		LF(s)	f	ano	Swisher (1992), sample 83CS-VV2A

*Age used in this study. Error as 1σ. All laser-fusion dates standardized to age of 27.84 Ma for Fish Canyon Tuff sanidine.
†Age reported in original source if different from age used in this study.
§K-Ar—potassium-argon age estimate. LF—$^{40}Ar/^{39}Ar$ laser-fusion age estimate. LF(s)—mean age of single grain analyses; LF(m)—mean age of multiple grain analyses.
#af—ash-flow tuff; f—fallout tuff.
**ano—anorthoclase; bi—biotite; fsp—feldspar, either a mix of plagioclase and sanidine or not specified; nr—not reported; pl—plagioclase: san—sanidine; wr—whole rock.

lation age estimates of the Ammonia Tanks and Rainier Mesa ash beds, calculated with reference to dated Gm ash beds, are concordant with $^{40}Ar/^{39}Ar$ age dates of correlative ash-flow tuffs. Although the estimates in Table 9 are among the most accurate, similar calculations for 18 other ash beds show average precisions of ± 0.06 m.y. (1σ); 14 of the 18 beds are within 0.10 m.y. of the average and all are within 0.20 m.y. of the average. Furthermore, during this investigation we estimated the age of 12 ash beds prior to dating by $^{40}Ar/^{39}Ar$ methods. For ash beds < 14 Ma our estimated ages were within 0.10 m.y. of the $^{40}Ar/^{39}Ar$ ages; for older ash beds, for which there are fewer available sections and control dates, estimated ages were within 0.25 m.y. of the $^{40}Ar/^{39}Ar$ ages. Thus, the interpolation and extrapolation error estimates in Figure 3 are given as ± 0.10 m.y. for beds <14 Ma or ± 0.25 m.y. for older beds, unless estimates from multiple sections or additional qualitative information indicate otherwise.

SOURCES OF TUFFS

As discussed previously, correlation of individual ash beds with specific ash-flow tuffs is an important dating method. Here we examine the broader topic of linking groups of ash beds with sources. Such links provide opportunities to use the vitric tuff record to assess patterns of explosive activity in various volcanic centers. Although the linking of a group of ash beds to a volcanic center is, of necessity, less definitive than correlation of ash beds to ash-flow tuffs, we believe that the available evidence supports such links for several groups of tuffs. We discuss the evidence in this section and comment briefly on likely sources for less common types of vitric tuffs.

TABLE 8. SUPPLEMENTARY DATA

Ash bed/unit*	Section	Age (Ma)†	Reported age (Ma)§	Analytical technique#	Dated Material**	Data sources/comments
Wolverine Creek	Arrow Canyon	7.2 ± 0.2	——	K-Ar	gl	Metcalf (1982)
Unnamed	El Paso basin	8.4 ± 1.8	——	FT	zir	Cox (1987), Loomis and Burbank (1988), Whistler and Burbank (1992)
CPT XIII	El Paso basin	10.4 ± 1.8	——	FT	zir	Cox (1987), Loomis and Burbank (1988), Whistler and Burbank (1992)
Basalt flow	El Paso basin	10.5 ± 0.25	——	K-Ar	nr	Whistler and Burbank (1992)
Ibex Peak 8	El Paso basin	11.8 ± 0.9	——	FT	zir	Cox (1987), Loomis and Burbank (1988), Whistler and Burbank (1992)
Coal Valley	Aldrich Station	11.1	10.8	K-Ar	bi	Evernden et al. (1964) sample KA 551
~Ammonia Tanks	Aldrich Station	11.5	11.2	K-Ar	bi	Evernden et al. (1964); sample KA 414
~Ammonia Tanks	Aldrich Station	10.8	10.5	K-Ar	bi	Evernden et al. (1964); sample KA 482
~Ammonia Tanks	Aldrich Station	11.5	10.2	K-Ar	bi	Evernden et al. (1964); sample KA 482II
~Ammonia Tanks	Aldrich Station	11.1	10.8	K-Ar	gl	Evernden et al. (1964); sample KA 500
Ammonia Tanks(?)	El Paso basin	10.3	10.0	K-Ar	bi	Evernden et al. (1964); sample KA 453
CPT IX	Stewart Valley	11.8	11.5	K-Ar	san	Evernden et al. (1964); sample KA 555
Rainier Mesa	Stewart Valley	11.0	——	K-Ar	bi	Evernden et al. (1964); sample KA 452
Rainier Mesa	Stewart Valley	11.74 ± 0.03	——	LF(s)	bi	Swisher (1992); Stewart Valley "Dated Tuff"
White Basin	White Basin	11.2 ± 1.1	——	FT	zir	Bohannon (1984); sample 27
~Overton Wash	Overton Wash	15.6 ± 0.9	——	FT	zir	Bohannon (1984); sample 30
~Overton Wash	Overton Wash	15.0 ± 0.8	——	FT	zir	Bohannon (1984); sample 39
Andesite lahar	Stewart Valley	15.25 ± 0.25	——	K-Ar	pl/hbl	Morton et al. (1977); sample 11920-2; average of two dates
<Andesite lahar	Stewart Valley	15.42 ± 0.17	——	K-Ar	pl	Swisher (1992); sample 86CS-MA1

*All units are ash beds except the andesite lahar and basalt flow. Symbol "~" indicates dated unit at approximate horizon of named unit. Symbol "<" indicates dated unit underlies named horizon.

†Error as 1σ. Laser-fusion dates standardized to age of 27.84 Ma for Fish Canyon Tuff sanidine. K-Ar dates standardized to constants of Steiger and Jäger (1977).

§Age reported in reference.

#K-Ar—potassium-argon age estimate. LF(s)—single grain $^{40}Ar/^{39}Ar$ laser-fusion age estimate.

**bi—biotite; gl—glass; hbl—hornblende; nr—not reported; pl—plagioclase; san—sanidine; wr—whole rock; zir—zircon.

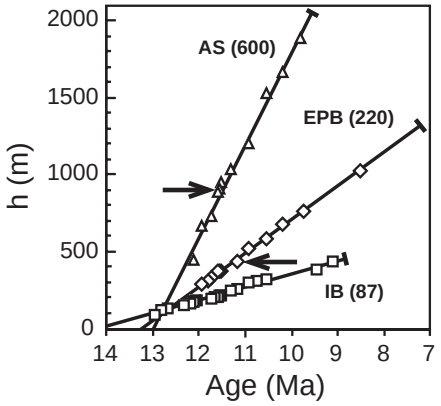

TABLE 9. INTERPOLATION/EXTRAPOLATION AGE ESTIMATES

Ash bed	Section/Age (Ma)				Mean age (Ma)	$^{40}Ar/^{39}Ar$ age (Ma)
	El Paso Basin	Aldrich Station	Stewart Valley	Ibapah Badlands		
Ammonia Tanks	11.57	11.49	11.54	11.53	11.53 ± 0.03	11.57 ± 0.05
Rainier Mesa	11.74	11.81	11.75	11.74	11.76 ± 0.03	11.72 ± 0.05
Tiva Canyon	——	——	——	12.91	——	12.83 ± 0.05
Yucca Mountain	——	——	——	12.92	——	N.A.

Note: Age estimates in individual sections are interpolation age estimates (Ammonia Tanks and Rainier Mesa ash beds) or extrapolation age estimates (Tiva Canyon and Yucca Mountain ash beds). Blank entries indicate ash bed not identified in section. Mean age is mean of the interpolation ages in the four sections. The error (1σ) is from the average variance in the interpolation ages and does not include errors in the control dates used for these ages. $^{40}Ar/^{39}Ar$ dates are from correlative ash-flow tuffs in the southwest Nevada volcanic field (SWNVF) (see Table 8); N.A.–not analyzed.

Figure 4. Sediment accumulation curves. Typical linear curves: AS—Aldrich Station section; EPB—El Paso basin section; IB—Ibapah Badlands section. Average accumulation rates (m/m.y.) are given in parentheses. Arrows point to positions of reported unconformities in EPB section (Whistler and Burbank, 1992) and AS section (Gilbert and Reynolds, 1973).

Snake River Plain Volcanic Province

A complex of northeastward-younging silicic volcanic centers, the Yellowstone hotspot track (Pierce and Morgan, 1992), marks the northern perimeter of the northern Basin and Range province. We group silicic volcanic centers of the hotspot track into the older (ca. 16.5–14.5 Ma) "Orevada" province on the west and the younger (<15 Ma) Snake River Plain volcanic province on the east (Fig. 1). The silicic rocks of the Snake River Plain volcanic province, discussed in this section, are predominantly metaluminous rhyolite ash-flow tuffs and lavas; those of the Orevada province, discussed later, include abundant peralkaline rhyolite ash-flow tuffs and lavas.

Analyses indicate that, with few exceptions, ash-flow tuffs and lavas from throughout the Snake River Plain volcanic province are within the compositional field of Gm tuffs and peralkaline tuffs are absent (Hughes et al., 1996). We have sampled and analyzed basal fallout tuffs of 23 Snake River Plain volcanic province ash-flow tuffs ranging in age from ca. 15 Ma to 5 Ma. With one exception all are Gm rhyolite tuffs. The exception is the 10.20 Ma Arbon Valley Tuff (Kellogg et al., 1994), a biotite-bearing Wm ash-flow tuff. Analyses for typical basal fallout tuffs of Snake River Plain volcanic province ash-flow tuffs as well as other proximal Snake River Plain volcanic province fallout tuffs were given in Perkins et al. (1995b).

Among the 117 Gm tuffs sampled in the northern Basin and Range basins, 96 lie within the compositional field of the basal Gm fallout tuffs of Snake River Plain volcanic province ash-flow tuffs. We informally refer to this subset of Gm tuffs as Snake River Plain–type Gm tuffs. Thirty-three of these 96 tuffs are correlative tuffs with 11 correlated to specific Snake River Plain volcanic

province ash-flow tuffs (Fig. 3). Thus, compositional characteristics provide both general and specific links of Snake River Plain–type tuffs to Snake River Plain volcanic province sources. Furthermore, Snake River Plain–type tuffs generally increase in frequency (tuffs/m.y.) and thickness towards the Snake River Plain with the maximum frequency and thickness occurring in the Trapper Creek section near the southern border of the Snake River Plain (Fig. 1). Together, the compositional characteristics and the geographic distribution patterns of frequency and thickness provide compelling evidence that most and probably all of the Snake River Plains-type tuffs had sources in the Snake River Plains volcanic province.

Southwestern Nevada Volcanic Field

The southwestern Nevada volcanic field, a major silicic volcanic center in the southern northern Basin and Range (Fig. 1), was active from ca. 16–7 Ma (Sawyer et al., 1994). Both peralkaline and metaluminous rhyolites were erupted from this center; the largest eruptions generated ash-flow tuffs that had volumes of 100–1200 km^3 (Sawyer et al., 1994). The metaluminous rhyolites of the southwestern Nevada volcanic field, which typically contain biotite (Warren et al., 1989), were erupted from ca. 16–10 Ma and include the most voluminous (200–1200 km^3) of the ash-flow tuffs. Correlation of four Wm tuffs with specific ash-flow tuffs in the southwestern Nevada volcanic field, discussed previously, establishes a direct tie between Wm tuffs and the southwestern Nevada volcanic field. In addition, most other typical Wm fallout tuffs have glass shards that are within the general compositional field of pumice glasses and aphyric metaluminous rhyolite lavas and ash-flow tuffs of the southwestern Nevada volcanic field (Broxton et al., 1989; Warren et al., 1989), and mostly are outside the compositional field of analyses of aphyric rhyolites reported from other major centers of middle to late Miocene silicic volcanism. Thus, on the basis of age and composition, the southwestern Nevada volcanic field is the likely source of many of the 50 Wm fallout tuffs we recognize in the interval from ca. 16–10 Ma.

Temporal and geographic distribution patterns also link Wm tuffs to the southwestern Nevada volcanic field. Figure 5 compares temporal patterns of metaluminous magma output in the southwestern Nevada volcanic field with the patterns of the thickness of Wm tuffs. The good correspondence between both patterns supports a southwestern Nevada volcanic field source for Wm tuffs. Furthermore, Wm tuffs are the dominant group of tuffs in sections within 250 km of the southwestern Nevada volcanic field for the period 13–11 Ma and, with the exception of the Ibapah Badlands section, such tuffs are rarely observed in sections north of latitude 40°N. This is the expected pattern for sources in the southwestern Nevada volcanic field. The compositional characteristics of the Wm tuffs and their temporal and geographic distribution patterns indicate that the southwestern Nevada volcanic field was the source for most Wm tuffs.

Orevada Volcanic Province

We group silicic volcanic centers at the west end of the Yellowstone hotspot track into the Orevada volcanic province (Fig. 1). They include the ca. 16.5–16 Ma High Rock caldera complex in northwestern Nevada (Ach and Swisher, 1990; Swisher, 1992), the ca. 16.5 to ca. 15 Ma McDermitt volcanic field along the Nevada-Oregon border (Rytuba and McKee, 1984; Swisher, 1992), and the ca. 15.6–14.5 Ma Lake Owyhee volcanic field along the Oregon-Idaho border (Rytuba and Vander Meulen, 1991). Ash-flow tuffs of the Orevada volcanic province are predominantly peralkaline rhyolites but include metaluminous rhyolites.

We tentatively link a distinctive group of older (>15.3 Ma) Gm tuffs, termed Buffalo Canyon–type Gm tuffs (Buffalo Canyon type), to sources in the Orevada province on the basis of age and geographic distribution. Buffalo Canyon–type tuffs are similar to Snake River Plain–type tuffs but have glass shards with a lower Th content (14–20 vs. 22–37 ppm), a lower Rb content (110–160 vs. 160–260 ppm), and a higher Zn content (76–134 vs. 30–78 ppm) than glass shards of Snake River Plain–type tuffs (content ranges represent the central 95% for each tuff type). There are 17 Buffalo Canyon–type tuffs that are recognized in the northern Basin and Range sections. Analyses of three typical Buffalo Canyon–type ash beds, the Huntington Creek 1, the Antonne Wash, and Virgin Valley 8 ash beds, are given in Tables 2 and 3. Buffalo Canyon–type tuffs are present in the Buffalo Canyon, Huntington Creek, Stewart Valley, Virgin Valley, and Willow Creek Reservoir sections in the northern part of the study area but appear to be absent in the coeval Overton Wash section in the southern part of the study area. Thus, a northern source is suggested. The Orevada volcanic province, which was active during the period in which Buffalo Canyon–type tuffs were deposited in northern Basin and Range sections, is the most likely source for these tuffs. From the limited information available on the composition of metaluminous rhyolites in this province, the Buffalo Canyon–type tuffs appear to be most similar to less evolved upper layers of ash-flow tuffs in the McDermitt volcanic field (Conrad, 1984). How-

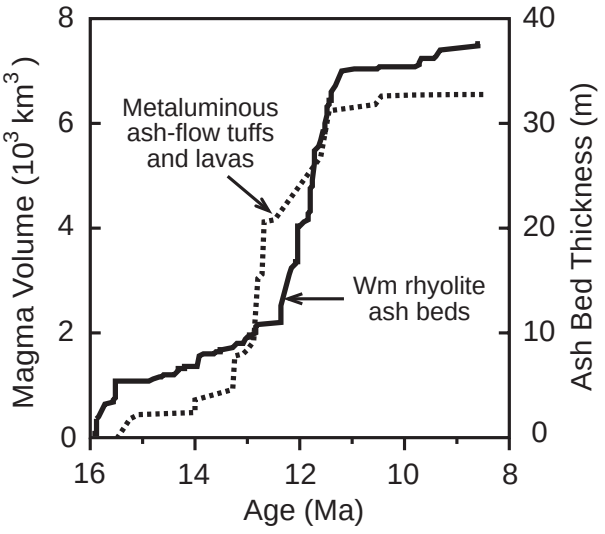

Figure 5. Cumulative thickness of distal Wm tuffs vs. cumulative volume of erupted metaluminous magma from the southwest Nevada volcanic field (SWNVF). Thickness of Wm tuffs is normalized to estimated thickness at 300 km from center of SWNVF. The estimated thickness at 300 km is $T_{300} \sim T_R\, e^{-K(R-300)}$, where T_R is measured thickness at R kilometers from the SWNVF and K = 0.0017 is an empirically estimated decay parameter. K is our best fit to data on thickness vs. distance to source for fallout ash beds of four large volume (=1000 km^3) pyroclastic eruptions—the Rainier Mesa, Ammonia Tanks, Huckleberry Ridge, and Lava Creek ash beds. Proximal metaluminous magma output for southwest Nevada volcanic field is from Sawyer et al. (1994).

ever, further work is needed to confidently identify the source(s) of Buffalo Canyon–type tuffs.

Other Sources

Sources for the other two tuff groups, the dacite tuffs and Gp tuffs, are not well established. In general the dacite tuffs have glass compositions similar to those of Quaternary dacite tuffs of the Cascade arc. In Miocene time, the western Cascade arc extended along the western margin of the northern Basin and Range (Christiansen and Yeats, 1992). It is likely that relatively small silicic eruptions within this dominantly andesitic arc produced many of the dacite tuffs. Several silicic volcanic centers are likely sources for the Gp tuffs. Peralkaline ash-flow tuffs and lavas are reported in the southwestern Nevada volcanic field, in the Kane Wash caldera complex, the Orevada volcanic province, and the Harney basin (Greene, 1973; Noble et al., 1970; Novak and Mahood, 1986; Rytuba and McKee, 1984; Rytuba and Vander Meulen, 1991; Sawyer et al., 1994). We link one Gp tuff to the southwestern Nevada volcanic field, the 13.78 Ma Grouse Canyon(?) ash bed. This ash bed is a good compositional and chronological match to the ca. 13.8 Ma comendites of the Belted Range Group of the southwestern Nevada volcanic field (Sawyer and Sargent, 1989; Sawyer et al., 1994). It may be the correlative of the 13.84 (13.70) ± 0.05 Ma Grouse Canyon Tuff, but correlation to some other unit of the Belted Range Group cannot be ruled out.

Three miscellaneous tuffs are tied to specific sources. First, a ca. 9 Ma unnamed potassium-rich dacite (i.e., latite) ash bed near the top of the Ibapah Badlands section has a glass shard composition similar to that of basal vitrophyre of the Tollhouse Member of the Eureka Valley Tuff in western Nevada. The 9–10 Ma Eureka Valley Tuff is in the Little Walker volcanic center of west-central Nevada (Fig. 1; Noble et al., 1976). Second, the Rattlesnake ash bed is an excellent match to basal fallout tuff we collected from the 7.05 Ma Rattlesnake Tuff (Streck and Grunder, 1995) in the Harney basin, Oregon (Fig. 3). The Rattlesnake Tuff, a miscellaneous Gm tuff, has a glass shard composition strikingly different from Snake River Plain–type Gm tuffs but in some ways similar to Buffalo Canyon–type Gm tuffs (i.e., low Rb and Th and high Mn contents in glass; see Table 3). Third, a ca. 6.7 Ma miscellaneous Wm lapilli tuff near the top of the Rush Valley section has glass with the high Rb, Th, and F contents characteristic of topaz rhyolite. The likely source was the nearby Thomas Range (Fig. 1), a center of 7–6 Ma topaz rhyolite volcanism (Lindsey et al., 1975).

DISCUSSION

Establishment of the sequence and age of vitric tuffs in the northern Basin and Range provides considerable information about space-time patterns of explosive volcanism and basin development in the region. Several examples illustrate the potential of using the northern Basin and Range vitric tuff database to address topics in volcanism and basin development in this region and in areas outside the province.

Pattern of Explosive Volcanism: Southwestern Nevada Volcanic Field

Sawyer et al. (1994) reported that explosive caldera forming volcanism in the southwestern Nevada volcanic field was episodic; brief periods of large volume ash-flow tuff eruptions were separated by intervals of relative quiescence. The overall pattern consisted of an initial period (ca. 16–14 Ma) of moderate magma output (~50 km^3/100 k.y.), a culminating period (ca. 14–11.5 Ma) of high magma output (160–2500 km^3/100 k.y.), and a waning period (ca. 11.5–7.5 Ma) of low magma output (15 km^3/100 k.y.). This pattern mainly reflects eruption of the volumetrically dominant metaluminous rhyolite magmas in the southwestern Nevada volcanic field. The pattern of cumulative thickness of Wm rhyolite tuffs, parallels that of cumulative volume of metaluminous ash-flow tuff and lava in the southwestern Nevada volcanic field, showing clearly the initial, culminating, and waning periods of magma output from this volcanic field (Fig. 5). However, the concept of strongly episodic volcanism inferred by Sawyer et al. (1994) is not apparent in the pattern of fallout tuff thickness. The sequence of Wm fallout tuffs is essentially continuous during the initial and culminating eruption periods. Furthermore, the four ash beds associated with the major metaluminous ash-flow tuffs in the southwestern Nevada volcanic field account for only a small proportion of cumulative thickness of Wm ash beds. We cannot yet calculate the volume of fallout ash from the southwestern Nevada volcanic field, but it must represent a significant component of magma output that needs to be considered in any comprehensive assessment of the southwestern Nevada volcanic field.

Characteristics of Northern Basin and Range Basins

Rates and Patterns of Sediment Accumulation. Rates of sediment accumulation in the northern Basin and Range basins vary by an order of magnitude from a low of 60–90 m/m.y. in the Ibapah and upper Buffalo Canyon sections to a high of ~600 m/m.y. in the Aldrich Station section. Some sections, like the El Paso basin section, had nearly constant rates of sediment accumulation over the interval for which we have age control. Other sections (e.g., Ibapah Badlands) show more scatter about the average accumulation rate, discrete intervals having higher or lower rates than average (Fig. 4). A few sections have distinctly different accumulation rates in different stratigraphic intervals. For example, the Buffalo Canyon section accumulated at ~300 m/m.y. in the lower part of the section but at only ~60 m/m.y. in the upper part of the section. The Trapper Creek section, as reported previously (Perkins et al., 1995b), has distinctly lower rates of sediment accumulation in the lower and upper parts of the section than in the middle of the section. These latter sections are composites with stratigraphic measurements made as much as 10 km apart, so observed variation in accumulation rates may reflect either temporal or geographic variation. Sampling in multiple sections within an individual basin is needed to sort out the temporal and geographic variation in sediment accumulation rates.

The average rate of sediment accumulation (~280 m/m.y.) and the range in rates of sediment accumulation in currently active northern Basin and Range basins are similar to those of the middle to late Miocene northern Basin and Range basins (Fig. 6). This suggests that older basins had rates of sediment input and tectonic subsidence roughly comparable to some currently active basins in the region.

Age and Pattern of Basin Initiation. Estimates of the ages of the oldest strata in northern Basin and Range basins sampled in this study are given in Table 10. These age estimates are extrapolated downward using sediment accumulation curves (Fig. 4). Error estimates for the age of the oldest strata are qualitative. In some basins, underlying volcanic rocks provide close bounds on the age of the oldest deposits and suggest that the extrapolated age estimates are reasonable (Table 10).

The Virgin Valley, Willow Creek, Huntington Creek, Buffalo Canyon, Stewart Valley, and Horse Spring basins appear to have been active by 16.5–15.5 Ma. These basins are within a north-trending belt in the central part of the northern Basin and Range (Fig. 1). Most basins east and west of this central belt were active by ca. 13 Ma, but the Pocatello, Cache Valley, and Salt Lake Valley basins along the northeast margin of the province were not active until ca. 11 to ca. 8 Ma. Thus, there is a suggestion that the northern Basin and Range basins become younger toward the western and eastern margins of the province. This pattern was noted by Stewart (1992) in the western part of the northern Basin and Range, and by Rodgers et al. (1990) in the northeastern part of

the northern Basin and Range. However, chronologic control on most northern Basin and Range basins is still limited, so it is still unclear whether the pattern is real or is an artifact of limited data.

Basin Duration. Our extrapolated age estimates of the youngest strata in northern Basin and Range basins are also listed in Table 10. Strata of most basins are overlapped unconformably by younger units, so these estimates should be regarded as lower bounds on the age of the youngest strata that may have once filled these basins. Dated volcanic rocks unconformably overlying the youngest strata in some basins provide bounds for the age of the youngest strata (Table 10).

On the basis of our age estimates of youngest and oldest strata, a typical northern Basin and Range basin was active for 5 to 6 m.y. For basins where there is good age control throughout the basin fill (Wassuk, Stewart Valley, Goose Creek, and Ibapah Badlands basins), sedimentation continued uninterrupted throughout the life of the basin. The Humboldt basin probably accumulated sediment continuously from 16 until at least 9.8 Ma, but a normal fault that cuts out strata between 11.5 and 9.8 Ma along Huntington Creek leaves some uncertainty about the continuity of sedimentation.

Unconformities have been proposed to be in the El Paso basin (Whistler and Burbank, 1992) and in the Aldrich station section (Gilbert and Reynolds, 1973), but we find no evidence of either the ~0.7 m.y. gap in the El Paso basin section at about 450 m or the proposed gap in the Aldrich Station section at ~800 m (Fig. 4). There may be an unconformity between the lower and upper sections in the Buffalo Canyon basin, but further work is needed to clarify relations between these sections.

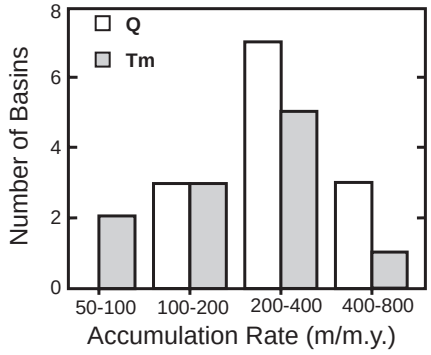

Figure 6. Average sediment accumulation rates. Tm—estimates for middle to late Miocene NBR (northern Basin and Range) basins sampled in this study. Q—estimate for active NBR basins to depth of Bishop ash bed or Lava Creek B ash bed. Data sources for Quaternary basins: Bonneville basin, Utah—9 values from 130–420 m/m.y., Moutoux (1995), Williams (1994); Mono basin, California—2 values of 215 and 540 m/m.y., Axtell (1972), Scholl et al. (1967); Owens Valley, California—410 m/m.y., Bischoff (1993).

Recognition of Fallout Tuffs Outside the Northern Basin and Range

The age and sequence of vitric tuffs in the northern Basin and Range will be useful in correlating strata throughout much of the western United States We briefly reported (Perkins and Nash, 1994; Perkins et al., 1995a; Powers and Holt, 1993, p. 272) on the correlation of Snake River Plain–type tuffs in the Teewinot Formation of northwest Wyoming, the Ash Hollow Formation of the northern Great Plains, and the Gatuña Formation of the southern Great Plains with northern Basin and Range tuffs. These correlations improve understanding of the age range and rates of sediment accumulation in these formations and also provide important information about distribution of fallout ash from major middle and late Miocene eruptions in the Snake River Plain volcanic province. Studies in progress on the Tesuque Formation in the Rio Grande Rift of New Mexico, the Browns Park and Troublesome formations of Colorado, the Sixmile Creek Formation of Montana, and the Trout Creek, Mascall and other Miocene Formations of Oregon show that northern Basin and Range tuffs are present throughout the intermontane west. Further studies will establish bed to bed correlations throughout the western United States. It is likely that, as in the case of some major Quaternary eruptions (Sarna-Wojcicki et al., 1987), some middle and late Miocene tuffs of the northern Basin and Range are also present in the eastern Pacific.

TABLE 10. ESTIMATED AGE RANGE OF BASINS

Section*/basin	Underlying strata/age (Ma)[#]	Oldest strata (Ma)[§]	Youngest strata (Ma)[§]	Overlying strata**/age (Ma)
EPB/El Paso basin	Tmv /15 -18	13.2 ± 0.5	7.0 ± 0.5	QTs
AS/Wassuk	Tmv /13	13.0 ± 0.5	9.0 ± 0.5	Tmv /~7
OW–WB/Horse Springs	Tmos /26-18	16.0–17.0	<11.0	Tmv / ~10
SV/Stewart Valley	Tmv	16.0 ± 0.5	10.0 ± 0.5	QTs
BC/Buffalo Canyon	Tmv /17-19	16.2 ± 0.5	10.0 ± 0.5	QTs
VV/Virgin Valley	Tmv /16.3	16.2 ± 0.3	<14.5 ± 0.5	Tms, Tmv
WC/Willow Creek	Tov /~32	16.5 ± 0.5	<15.5	QTs
HTC/Humboldt	Tes	16.0 ± 0.3	<9.8	QTs
TC/Goose Creek	Pz	14.0 ± 0.1	8.5 ± 0.5	Tmv / 7.3
IB/Deep Springs	Tev /~39	14.2 ± 0.5	8.5 ± 0.5	QTs
RV/Rush Valley	unknown	>10	<6.7	QTs
P-CV-JN[†]	Pz-Tes-Tev	10.0–8.0	7.5–6.0	QTs

*Section abbreviations same as in Figure 1.
[†]Only reconnaissance sampling in these sections; age ranges are rough estimates.
[#]Tmv, Tms—Miocene volcanic or sedimentary rocks; Tmos—Miocene to Oligocene sedimentary rocks; Tov—Oligocene volcanic rocks: Tev, Tes—Eocene volcanic or sedimentary rocks; Pz—Paleozoic sedimentary rocks.
[§]Symbol "<" indicates lower bound–younger strata present but not sampled in this study. Symbol ">" indicates upper bound–older strata believed present but covered.
**QTs—undifferentiated late Neogene alluvial deposits. Typically flat lying or very gently tilted.

SUMMARY AND CONCLUSIONS

Vitric fallout tuffs and their reworked equivalents are a characteristic constituent of middle to late Miocene sedimentary basins in the northern Basin and Range province. Applying correlation techniques used in correlating Quaternary ash beds, we show that these vitric tuffs are uniquely characterized by glass shard composition, relative stratigraphic position, and age. Our detailed sampling and analyses indicate there are at least 213 different vitric tuffs in these basins. About 45% of these are nonperalkaline gray vitric tuffs from sources in the Snake River Plain volcanic province of southern Idaho and adjacent states. Another 34% of the tuffs are white biotitic tuffs, most of which were probably from sources in the southwestern Nevada volcanic field. Thus ~80 % of the tuffs come from two major silicic volcanic centers. The remaining tuffs, mainly peralkaline rhyolite tuffs and dacite tuffs, also appear to be from sources within or adjacent to the northern Basin and Range province, although specific sources are generally unknown.

Of the 213 different tuffs we have identified in the middle to late Miocene sedimentary basins of the northern Basin and Range province, 59 correlate between two or more basins, or between the basins and proximal ash-flow tuffs. Using these 59 correlative tuffs, we have established a composite sequence of vitric tuffs spanning ca. 16 to ca. 6 Ma. We also have established relatively high

precision age estimates for these tuffs by a combination of direct isotopic dating of the fallout tuffs, correlation to isotopically dated ash-flow tuffs, and linear interpolation and extrapolation referenced to isotopically dated tuffs. With the completion of this study a database is available to investigate facets of middle to late Miocene explosive volcanism and basin development within and beyond the northern Basin and Range.

ACKNOWLEDGMENTS

We thank Andrei Sarna-Wojcicki (U.S. Geological Survey, Menlo Park, California) for the loan of Bill Eastwood's samples from the Wassuk basin. We also thank Carl Swisher III (Berkeley Geochronology Center) for samples and stratigraphic information on several tuffs he dated, and Laurie Brown, Anita Grunder, and Sheila Seaman for their reviews and comments, which improved the manuscript. This work was supported by National Science Foundation grants EAR-9204700 and EAR-9316289 and by the Mineral Leasing Fund of the State of Utah.

APPENDIX A. LOCATIONS OF DATED SAMPLES AND MEASURED SECTIONS

Samples

tw94–672. Faust ash bed. The sample was collected from the base of a >3-m-thick fallout tuff in the Teewinot Formation north of Jackson, Wyoming. This ash bed is at the west end of the Haybarn Hill section of Love (1975) and just above the horizon of sample KA929 of Evernden et al. (1964). Gros Ventre Junction quadrangle (7.5′), Wyoming, 43°33.96′N, 110°46.74′W, elevation 1969 ± 6 m (6460 ± 20 ft).

tc90–26. Base-surge deposit of tuff of McMullen Creek (unit 1?). The sample was collected near top of 6.6-m-thick base-surge deposit. This unit was identified as tuff of the Wooden Shoe Butte in the lower Trapper Creek section of Perkins et al. (1995b). Oakley quadrangle (7.5′), Idaho, 42°10.71′N, 113°57.76′W, elevation 1518 ± 6 m (4980 ± 20 ft).

wjr93–436. CPT V ash bed. The sample was collected from a 3.6-m-thick basal fallout tuff that underlies Cougar Point Tuff unit V. This ash bed is exposed in the canyon of the Jarbidge River in a small borrow quarry along the east side of the road, about 1.2 km north of turnoff onto Deer Creek Road, Jarbidge North quadrangle (7.5′), Nevada, 41°56.74′N, 115°24.98′W, elevation 1719 ± 12 m (5640 ± 40 ft).

tc89–18a. CPT V ash bed. The sample was collected from base of a 13-m-thick fallout tuff in the tuff of Ibex Peak of Mytton et al. (1990). This ash bed is in the Ibex Hollow and vicinity section of Perkins et al. (1995b) and is the lowest unit in a cliff-forming sequence of fallout tuff and reworked fallout tuff capped by dark gray nonwelded ash-flow tuff (tuff of Ibex Hollow). Severe Springs quadrangle (7.5′), Idaho, 42°07.53′N, 114°04.11′W, elevation 1695 ± 12 m (5560 ± 40 ft).

CPT III. CPT III vitrophyre. The sample was collected from the 5.5-m-thick basal vitrophyre of Cougar Point Tuff unit III in an exposure along the east side of the Bruneau River canyon, Nevada, near the confluence with McDonald Creek. Exposure is shown in Figure 3 of Bonnichsen and Citron (1982). Big Table quadrangle (7.5′), Nevada-Idaho, 41°58.07′N, 115°40.00′W, elevation 1524 ± 12 m (5000 ± 40 ft).

sv92–94a. Grouse Canyon? ash bed. The sample was collected from the base of a 3 cm thick fallout tuff in Stewart Valley, Nevada, near the base of unit S4 of the Savage Canyon Formation of Schorn et al. (1989). Granny Goose Well quadrangle (7.5′), Nevada, 38°39.92′N, 117°58.90′W, elevation 1612 ± 6 m (5290 ± 20 ft).

sv93–404. Paradise Valley ash bed. The sample was collected from a 50 cm thick reworked tuff in the lower part of unit S1 of the Savage Canyon Formation of Schorn et al. (1989). Stewart Spring quadrangle (7.5′), Nevada, 38°32.43′N, 117°57.05′W, elevation 1865 ± 12 m (6120 ± 40 ft).

buf94–618. Paradise Valley ash bed. The sample was collected from a lens of "pure" tuff at the base of a 180-cm-thick reworked tuff near the top of member 3 of the Buffalo Canyon Formation (Axelrod, 1991). Buffalo Summit quadrangle (7.5′), Nevada, 39°13.20′N, 117°47.71′W, elevation 1868 ± 6 m (6130 ± 20 ft).

buf94–622. The sample was collected from the base of a 10-cm-thick fallout tuff in Buffalo Canyon, Nevada. This ash bed is in the upper part of the member 2 of the Buffalo Canyon Formation (Axelrod, 1991). Buffalo Summit quadrangle (7.5′), Nevada, 39°12.16′N, 117°47.67′W, elevation 1878 ± 6 m (6160 ± 20 ft).

Sections

Aldrich Station Section. Westward from east edge of sec. 6, T.7N., R.28E. to west edge of sec. 2, T.7N., R.27E., Ninemile Ranch quadrangle, Nevada. Same as Aldrich Station section of Axelrod (1956) and Eastwood (1969).

Arrow Canyon Section. Northeast face of Table Mountain in south-central Wildcat Wash, SE quadrangle, Nevada. In "Badlands" area of Metcalf (1982).

Buffalo Canyon Sections. Lower section in and around sections 27 and 34, T.16N., R.37E., Buffalo Summit quadrangle, Nevada. Upper section in south-central part of section 8 and north-central part of section 17, T.16N., R.37E., Desatoya Peak quadrangle, Nevada.

Burns, Oregon, "Section." Several localities in the Harney basin north of Burns, Oregon, including basal fallout tuffs of Rattlesnake Tuff and tuff of Devine Canyon (Streck and Grunder, 1995; Greene, 1973).

Cache Valley Sections. Composite of several sections in and around Cache Valley, Utah-Idaho, including the Cache Valley, Cub River, and Mink Creek sections of Smith (1975).

Chalk Hills Section. NW1/4 SW1/4 of Sec. 19, T.7S., R.4E. of the Chalk Hills quadrangle, Idaho. Section 14 of Kimmel (1979).

El Paso Basin Section. Lower part of the section along west side of Last Chance Canyon in the vicinity of Cudahys Old Dutch Cleanser Mine, Saltdale NW quadrangle, California. Upper part of section from east edge of section 24 northwestward into section 11, T.29S., R.37E., Saltdale NW quadrangle, California. Same as section F and upper part of section E of Whistler and Burbank (1992).

Ferry Hollow Section. In Ferry Hollow southwest of American Falls, Idaho, NW1/4 sec. 6, T.8S., R.31E., American Falls SW quadrangle, Idaho. Type area of Walcott Tuff (Walcott Formation) of Stearns and Isotoff (1956).

Hazen Section. Open-pit diatomite mines in sections 8, 17, and 18, T.19N., R.26E., Hazen, Nevada, quadrangle. Composite of sections of Brown (1986).

Huntington Creek Section. Along east side of Huntington Creek from NE1/4 sec. 1, T.31N., R.35E. southward into SW1/4 sec. 18, T.31N., R.36E., West of Lee quadrangle, Nevada. Same as reference section of the Humboldt Formation (restricted) of Smith and Ketner (1976).

Ibapah Badlands Section. Lower part of section exposed in the southwestern part of the Ferber Peak NW quadrangle, Nevada. Upper part of section exposed in sec. 21 and south-central part of sec. 16, T.26N., R.70E., Ferber Peak SE quadrangle, Nevada-Utah.

Jordan Narrows Section. Section of Smith (1975) along Jordan River in sec. 26, T.4S., R.1W., Jordan Narrows quadrangle, Utah.

Overton Wash Section. Along Overton Wash in the southwestern corner of Overton quadrangle, Nevada. Sequence of strata between Overton Wash Conglomerate and Muddy Creek Formation.

Pahranagat Valley Section. East-central part of sec. 27, T.7S., R.61E., Alamo SE, quadrangle, Nevada. Pahranagat Valley area of Metcalf (1982).

Pocatello Section. Composite from several areas near Pocatello, Idaho.

Ririe Reservoir. Section above boat ramp in Blacktail Deer Recreation Area in SW1/4 sec. 16 and SE1/4 sec. 17, T.2N., R.40E., Rigby SE quadrangle, Idaho. Section described in field guide of Hackett and Morgan (1988), but note that a ca. 6 Ma Miocene ash-flow tuff near top of this section was incorrectly identified as the 2.06 Ma Huckleberry Tuff by these workers.

Rush Valley Section. Faust and Vernon NE quadrangles, Utah, in sections 26 and 27, T.7S., R.5W. Same as Rush Valley section of Smith (1975).

South Willow Canyon Section. Deseret Peak East and North Willow Canyon quadrangles from sec. 6, T.4S., R.6W. northeastward into sec. 33, T.3S., R.6W.

Stewart Valley Section. Lower half of section in the NE 1/4 of the SW 1/4 of the Stewart Springs quadrangle, Nevada. Upper half of section generally in northern part of SW 1/4 of the Granny Goose Well quadrangle, Nevada, in area northeast of Stewart Valley Road and along Stewart Valley Road in southern part of this quadrangle.

Succor Creek Section. East half of sec. 32 and west half of sec. 31, T.23S., R.45E., Owyhee Ridge quadrangle, Oregon. Same as Devils Gate section of Downing (1992).

Thousand Creek Section. Along north side of Highway 140 in area west-northwest of Thousand Creek Ranch, Thousand Creek Gorge quadrangle, Nevada. Mostly in NE1/4 sec. 22, T.46N., R.26E.

Trapper Creek Section. Same as composite Trapper Creek section of Perkins et al. (1995b).

Virgin Valley Section. Composite of a number of partial sections along Virgin Valley from vicinity of Virgin Valley Ranch northward to Thousand Creek; i.e., from 41°47.97′N, 119°05.60′W to 41°52.16′N, 119°01.45′W.

White Basin Section. In the general vicinity of 36°20.0′N, 114°40.0′W, Muddy Peak quadrangle, Nevada.

Willow Creek Section. NE1/4 of sec. 27 and extreme western part of sec. 26, T.39N., R.48E., Willow Creek Reservoir quadrangle, Nevada. Only lower part of section sampled, up a to welded ash-flow tuff along east edge of section 26.

APPENDIX B. STANDARDIZATION OF $^{40}Ar/^{39}Ar$ DATES

The primary standard used as an Ar monitor in $^{40}Ar/^{39}Ar$ dating is the hornblende MMhb–1. At the Geochronology Laboratory of the U.S. Geological Survey, Menlo Park, California, the assigned age of Mmhb–1 is 513.9 Ma (Dalrymple et al., 1993); at the Berkeley Geochronology Center, Berkeley, California,

and the New Mexico Geochronology Research Laboratory, Socorro, the assigned age is 520.4 Ma, as reported by Sampson and Alexander (1987). With reference to MMhb-1, the Menlo Park laboratory dates Fish Canyon Tuff sanidine (the monitor for $^{40}Ar/^{39}Ar$ analyses at the Socorro and Berkeley laboratories) as 27.55 Ma, but the other laboratories assign an age of 27.84 Ma to this monitor. This difference of ~1% is significant because precision of the $^{40}Ar/^{39}Ar$ laser-fusion ages is commonly better than ± 0.5% (1σ). To improve consistency among the $^{40}Ar/^{39}Ar$ dates, we have increased Menlo Park dates by 1.0105 (i.e., 27.84/27.55).

REFERENCES CITED

Ach, J. A., and Swisher, C. C., 1990, The High Rock caldera complex; nested "failed" calderas in northwestern Nevada: Eos (Transactions, American Geophysical Union), v.71, p. 1614.

Axelrod, D. I., 1956, Mio-Pliocene floras from west-central Nevada: University of California Publications in the Geological Sciences, v. 33, 322 p.

Axelrod, D. I., 1991, The early Miocene Buffalo Canyon flora of western Nevada: University of California Publications in the Geological Sciences, v. 135, 76 p.

Axtell, L. H., 1972, Mono Lake geothermal wells abandoned: California Geology, v. 25, p. 66–67.

Bischoff, J. L., 1993, Age-depth relations for the sediment column at Owens Lake, California; OL-92 drill hole: U.S. Geological Survey Open-File Report OF 93–0683, p. 251–260.

Bohannon, R. G., 1984, Nonmarine sedimentary rocks of Tertiary age in the Lake Mead region, southeastern Nevada and northwestern Arizona: U.S. Geological Survey Professional Paper 1259, 72 p.

Bonnichsen, B., 1982, Cougar Point Tuff, southwestern Idaho and vicinity, *in* Bonnichsen, B., and Breckenridge, R. M., eds., Cenozoic geology of Idaho: Idaho Bureau of Mines and Geology Bulletin 26, p. 237–254.

Bonnichsen, B., and Citron, G. P., 1982, The Bruneau-Jarbidge eruptive center, southwestern Idaho, *in* Bonnichsen, B., and Breckenridge, R. M., eds., Cenozoic geology of Idaho: Idaho Bureau of Mines and Geology Bulletin 26, p. 255–280.

Brown, F. H., 1986, Report on correlation of quarries in the Hazen area by chemical analysis of tephra layers: Final Technical Report for National Science Foundation Contract 431–2681–A, 23 p.

Broxton, D. E., Warren, R. G., and Byers, F. M., 1989, Chemical and mineralogic trends within the Timber Mountain–Oasis Valley caldera complex, Nevada: Evidence for multiple cycles of chemical evolution in a long-lived silicic magma system: Journal of Geophysical Research, v. 94, p. 5961–5985.

Burbank, D. W., and Whistler, D. P., 1987, Temporally constrained tectonic rotations derived from magnetostratigraphic data: Implications for the initiation of the Garlock fault: Geology, v. 15, p. 1172–1175.

Christiansen, R. L., and Yeats, R. S., 1992, Post-Laramide geology of the U.S. Cordilleran region, *in* Burchfield, B. C., Lipman, P. C., and Zoback, M. L., eds., The Cordilleran orogen: Conterminous U.S.: Boulder, Colorado, Geological Society of America, Geology of North America, v. G-3, p. 261–406.

Coats, R. R., 1987, Geology of Elko County, Nevada: Nevada Bureau of Mines and Geology Bulletin 101, 112 p.

Conrad, 1984, The mineralogy and petrology of compositionally zoned ash flow tuffs, and related silicic volcanic rocks, from the McDermitt caldera complex, Nevada-Oregon: Journal of Geophysical Research, v. 89, p. 8639–8644.

Cox, B. F., 1987, Basin analysis and paleontology of the Paleocene and Eocene Goler Formation, El Paso Mountains, California: Society of Economic Paleontologists and Mineralogists Guidebook 57, p. 1–30.

Dalrymple, G. B., Izett, G. A., Snee, L. W., and Obradovich, J. D., 1993, $^{40}Ar/^{39}Ar$ spectra and total-fusion ages of tektites from Cretaceous-Tertiary rocks in the Beloc Formation, Haiti: U.S. Geological Survey Bulletin 2065, 20 p.

Downing, K. F., 1992, Biostratigraphy, taphonomy, and paleoecology of vertebrates from the Sucker Creek Formation (Miocene) of southeastern Oregon [Ph.D. thesis]: Tucson, University of Arizona, 495 p.

Downing, K. F., and Swisher, C. C., III, 1993, New $^{40}Ar/^{39}Ar$ dates and refined geochronology of the Sucker Creek Formation, Oregon [abs.]: Journal of Vertebrate Paleontology, v. 13, no. 3, p. 33A.

Eastwood, W. C., 1969, Trace element correlation of Tertiary volcanic ashes from western Nevada [Master's thesis]: Berkeley, University of California, 89 p.

Evernden, J. F., Savage, D. E., Curtis, G. H., and James, G. T., 1964, Potassium-argon dates and the Cenozoic mammalian chronology of North America: American Journal of Science, v. 262, p. 145–198.

Flood, T. P., Vogel, T. A., and Schuraytz, B. C., 1989, Chemical evolution of a magmatic system: The Paintbrush Tuff, southwestern Nevada volcanic field: Journal of Geophysical Research, v. 94, p. 5943–5960.

Gilbert, C. M., and Reynolds, M. W., 1973, Character and chronology of basin development, western margin of the Basin and Range province: Geological Society of America Bulletin, v. 84, p. 2489–2510.

Golia, R. T., and Stewart, J. H., 1984, Depositional environments and paleogeography of the upper Miocene Wassuk Group, west central Nevada: Sedimentary Geology, v. 38, p. 159–180.

Greene, R. C., 1973, Petrology of the welded tuff of Devine Canyon, southeastern Oregon: U.S. Geological Survey Professional Paper 797, 26 p.

Greene, R. C., 1984, Geologic appraisal of the Charles Sheldon wilderness study area, Nevada and Oregon, *in* U.S. Geological Survey and U.S. Bureau of Mines, Mineral Resources of the Charles Sheldon wilderness study area, Humboldt and Washoe counties, Nevada, and Lake and Harney counties, Oregon: U.S. Geological Survey Bulletin 1538, p. 13–34.

Gregory, K. M., and McIntosh, W. C., 1996, Paleoclimate and paleoelevation of the Oligocene Pitch–Pinnacle flora, Sawatch Range, Colorado: Geological Society of America Bulletin, v. 108, p. 545–561.

Hackett, W. R., and Morgan, L. A., 1988, Explosive basaltic and rhyolitic volcanism of the eastern Snake River Plain, Idaho, *in* Link, P. K., and Hackett, W. R., eds., Guidebook to the geology of central and southern Idaho: Idaho Geological Survey Bulletin 27, p. 283–301.

Heylmun, E. B., 1965, Reconnaissance of the Tertiary sedimentary rocks in western Utah: Utah Geological and Mineralogical Survey Bulletin 75, 38 p.

Hintze, L. F., 1988, Geologic history of Utah, Kowallis, B. J., series ed., Provo, Utah, Brigham Young University Geology Studies Special Publication 7, 202 p.

Hughes, S. S., Parker, J. L., Watkins, A. M., and McCurry, M., 1996, Geochemical evidence for a magmatic transition along the Yellowstone hotspot track, *in* Hughes, S. S., and Thomas, R. C., eds., Geology of the crook in the Snake River Plain, Twin Falls and vicinity, Idaho: Northwest Geology, v. 26, p. 63–80.

Izett, G. A., 1981, Volcanic ash beds: Recorders of upper Cenozoic silicic pyroclastic volcanism in the western United States: Journal of Geophysical Research, v. 86, p. 10200–10222.

Kellogg, K. S., Harlan, S. S., Mehnert, H. H., Snee, L. W., Pierce, K. L., Hackett, W. R., and Rodgers, D. W., 1994, Major 10.2-Ma rhyolitic volcanism in the eastern Snake River Plain, Idaho: Isotopic age and stratigraphic setting of the Arbon Valley Tuff Member of the Starlight Formation: U.S. Geological Survey Bulletin 2091, 18 p.

Kimmel, P. G., 1979, Stratigraphy and paleoenvironments of the Miocene Chalk Hills Formation and Pliocene Glenns Ferry Formation in the western Snake River Plain, Idaho [Ph.D. thesis]: Ann Arbor, University of Michigan, 331 p.

Kimmel, P. G., 1982, Stratigraphy, age, and tectonic setting of the Miocene-Pliocene lacustrine sediments of the western Snake River Plain, Oregon and Idaho, *in* Bonnichsen, B., and Breckenridge, R. M., eds., Cenozoic geology of Idaho: Idaho Bureau of Mines and Geology Bulletin 26, p. 559–578.

Lenz, P. E., and Morris, C. L., 1993, Diatomite in Nevada: Society for Mining, Metallurgy, and Exploration, Inc., preprint no. 93–93, 11 p.

Lindsey, D. A., Naeser, C. W., and Shawe, D. R., 1975, Age of volcanism, intrusion, and mineralization in the Thomas Range, Keg Mountain, and Desert Mountain, western Utah: U.S. Geological Survey Journal of Research, v. 3, p. 597–604.

Loomis, D. P., and Burbank, D. W., 1988, The stratigraphic evolution of the El Paso Basin, southern California: Implications for the Miocene development of the Garlock fault and uplift on the Sierra Nevada: Geological Society of America Bulletin, v. 100, p. 12–28.

Love, J. D., 1975, Geologic map of the Gros Ventre Junction quadrangle, Teton County, Wyoming: U.S. Geological Survey Open-File Report 75–334, scale 1:24,000.

Luedke, R. G., and Smith, R. L., 1981, Map showing distribution, composition, and age of late Cenozoic volcanic centers in California and Nevada: U.S. Geological Survey Miscellaneous Investigations Series Map I-1091-C, scale 1:1 000 000.

Luedke, R. G., and Smith, R. L., 1982, Map showing distribution, composition, and age of late Cenozoic volcanic centers in Oregon and Washington: U.S. Geological Survey, Miscellaneous Investigations Series Map I-1091-D, scale 1:1 000 000.

Luedke, R. G., and Smith, R. L., 1983, Map showing distribution, composition and age of late Cenozoic volcanic centers, in Idaho, western Montana, west-central South Dakota, and northwestern Wyoming: U.S. Geological Survey Miscellaneous Investigations Map I-1091-E, scale 1:1 000 000.

Metcalf, L. A., 1982, Tephrostratigraphy and potassium-argon age determinations of seven volcanic ash layers in the Muddy Creek Formation of southern Nevada: Water Resources Center, Desert Research Institute, University of Nevada System, Publication 45023, 172 p.

Morgan, L. A., 1992, Stratigraphic relations and paleomagnetic and geochemical correlations of ignimbrites of the Heise volcanic field, eastern Snake River Plain, eastern Idaho and western Wyoming, *in* Link, P. K., Kuntz, M. A., and Platt, L. B., eds., Regional geology of eastern and western Wyoming: Geological Society of America Memoir 179, p. 215–225.

Morton, J. L., Silberman, M. L., Bonham, H. F., Jr., Garside, L. J., and Noble, D. C., 1977, K-Ar ages of volcanic rocks, plutonic rocks, and ore deposits in Nevada and eastern California: Determinations run under the USGS-NBMG cooperative program: Isochron/West, v. 20, p. 19–29.

Moutoux, T. E., 1995, Palynological and tephra correlations among deep wells in the modern Great Salt Lake, Utah, U.S.A.—Implications for Neogene through Pleistocene climatic reconstructions [Master's thesis]: Tucson, University of Arizona, 30 p.

Mytton, J. W., Williams, P. L., and Morgan, W. A., 1990, Geologic map of the Stricker 4 quadrangle, Cassia, Twin Falls, and Jerome Counties, Idaho: U.S. Geological Survey Miscellaneous Investigations Series Map I-2052, scale 1:48 000.

Naeser, C. W., Bryant, B., Crittenden, M. D., Jr., and Sorensen, M. L., 1983, Fission–track ages of apatite in the Wasatch Mountains, Utah: An uplift study, *in* Miller, D. M., Todd, V. R., and Howard, K. A., eds., Tectonic and stratigraphic studies in the eastern Great Basin: Geological Society of America Memoir 157, p. 29–36.

Nash, W. P., 1992, Analysis of oxygen with the electron microprobe: Application to hydrous glass and minerals: American Mineralogist, v. 77, p. 453–457.

Noble, D. C., McKee, E. H., Smith, J. G., and Korringa, M. K., 1970, Stratigraphy and geochronology of Miocene volcanic rocks in northwestern Nevada: U.S. Geological Survey Professional Paper 700D, p. D23–D32.

Noble, D. C., Korringa, M. K., Church, S. E., Bowman, H. R., Silberman, M. L., and Heropoulos, C. E., 1976, Elemental and isotopic geochemistry of nonhydrated quartz latite glasses from the Eureka Valley Tuff, east-central California: Geological Society of America Bulletin, v. 87, p. 754–762.

Novak, S. W., and Mahood, G. A., 1986, Rise and fall of a basalt-trachyte-rhyolite magma system at the Kane Springs Wash caldera, Nevada: Contributions to Mineralogy and Petrology, v. 94, p. 352–373.

Perkins, M. E., and Nash, W. P., 1994, Tephrochronology of the Teewinot Formation, Jackson Hole, Wyoming: Geological Society of America Abstracts with Programs, v. 26, no. 1, p. 58–59.

Perkins, M. E., Diffendal, R. F., Jr., and Voorhies, M. R., 1995a, Tephrochronology of the Ash Hollow Formation (Ogal-

lala Group)—Northern Great Plains: Geological Society of America Abstracts with Programs, v. 27, no. 3, p. 79.
Perkins, M. E., Nash, W. P., Brown, F. H., and Fleck, R. J., 1995b, Fallout tuffs of Trapper Creek, Idaho—A record of Miocene explosive volcanism in the Snake River Plain volcanic province: Geological Society of America Bulletin, v. 107, p. 1484–1506.
Pierce, K. L., and Morgan, L. A., 1992, The track of the Yellowstone hot spot: Volcanism, faulting, and uplift, *in* Link, P. K., Kuntz, M. A., and Platt, L. B., eds., Regional geology of eastern and western Wyoming: Geological Society of America Memoir 179, p. 1–53.
Powers, D. W., and Holt, R. M., 1993, The upper Cenozoic Gatuña Formation of southeastern New Mexico, *in* Carlsbad region, New Mexico and west Texas: New Mexico Geological Society, 44th Field Conference Guidebook, p. 271–282.
Rodgers, D. W., Hackett, W. R., and Ore, H. T., 1990, Extension of the Yellowstone Plateau, eastern Snake River Plain, and Owyhee Plateau: Geology, v. 18, p. 1138–1141.
Rytuba, J. J., and McKee, E. H., 1984, Peralkaline ash flow tuffs and calderas of the McDermitt volcanic field, southeast Oregon and north central Nevada: Journal of Geophysical Research, v. 89, p. 8616–8628.
Rytuba, J. J., and Vander Meulen, D. B., 1991, Hot-spring precious-metal systems in the Lake Owyhee volcanic field, Oregon-Idaho, *in* Raines, G. L., Lisle, R. E., Schafer, R. W., and Wilkinson, W. H., eds., Geology and ore deposits of the Great Basin, Symposium Proceedings: Reno, Geological Society of Nevada, p. 1085–1096.
Sampson, S. D., and Alexander, E. C., 1987, Calibration of the interlaboratory $^{40}Ar/^{39}Ar$ dating standard, MMhb–1: Chemical Geology, v. 66, p. 27–34.
Sarna-Wojcicki, A. M., and Davis, J. O., 1991, Quaternary tephrochronology, *in* Morrison, R. B., ed., Quaternary nonglacial geology, conterminous U.S.: Boulder, Colorado, Geological Society of America, Geology of North America, v. K-2, p. 93–116.
Sarna-Wojcicki, A. M., Morrison, S. D., Meyer, C. E., and Hillhouse, J. W., 1987, Correlation of upper Cenozoic tephra layers between sediments of the western United States and eastern Pacific Ocean, and comparison with biostratigraphic and magnetostratigraphic age data: Geological Society of America Bulletin, v. 98, p. 207–223.
Sawyer, D. A., and Sargent, K. A., 1989, Petrologic evolution of divergent peralkaline magmas from the Silent Canyon caldera complex: Journal of Geophysical Research, v. 94, p. 6021–6040.
Sawyer, D. A., Fleck, R. J., Lanphere, M. A., Warren, R. G., Broxton, D. E., and Hudson, M. R., 1994, Episodic caldera volcanism in the Miocene southwestern Nevada volcanic field: Revised stratigraphic framework, $^{40}Ar/^{39}Ar$ geochronology, and implications for magmatism and extension: Geological Society of American Bulletin, v. 106, p. 1304–1318.
Scholl, D. W., Von Huene, R., St.-Amand, P., and Ridlon, J. B., 1967, Age and origin of topography beneath Mono Lake, a remnant Pleistocene lake, California: Geological Society of America Bulletin, v. 78, p. 583–600.
Schorn, H. E., Scudder, H. I., Savage, D. E., and Firby, J. R., 1989, General stratigraphy and paleontology of the Miocene continental sequence in Stewart Valley, Mineral County, Nevada, U.S.A., *in* Liu, Gengwu, Tsuchi, Ryuichi, and Lin, Qibin, eds., Proceedings of International Symposium of Pacific Neogene Continental and Marine Events, National Working Group of China for IGCP-246: Nanjing, China, Nanjing University Press, p. 157–173.
Smith, J. F., Jr., and Ketner, K. B., 1976, Stratigraphy of post-Paleozoic rocks and summary of resources in the Carlin–Pinon Range area, Nevada: U.S. Geological Survey Professional Paper 867–B, 48 p.
Smith, R. P., 1975, Geochemistry of volcanic ash in the Salt Lake Group, Bonneville basin, Utah, Idaho, and Nevada [Master's thesis]: Salt Lake City, University of Utah, 93 p.
Smith, R. P. and Nash, W. P., 1976, Chemical correlation of volcanic ash deposits in the Salt Lake Group, Utah, Idaho and Nevada: Journal Sedimentary Petrology, v. 46, p. 930–939.
Stearns, H. T., and Isotoff, A., 1956, Stratigraphic sequence in Eagle Rock volcanic area near American Falls, Idaho: Geological Society of America Bulletin v. 67, p. 19–34.
Steiger, R. H., and Jäger, E., 1977, Subcommission on geochronology: Convention on the use of decay constants in geo- and cosmochronology: Earth and Planetary Science Letters, v. 36, p. 359–362.
Stewart, J. H., 1992, Paleogeography and tectonic setting of Miocene continental strata in the northern part of the Walker Lane Belt, *in* Craig, S. D., ed., Structure, tectonics and mineralization of the Walker Lane: Reno, Geological Society of Nevada, Walker Lane Symposium Proceedings, p. 53–61.
Streck, M. J., and Grunder, A. L., 1995, Crystallization and welding variations in a widespread ignimbrite sheet; the Rattlesnake Tuff, eastern Oregon, USA: Bulletin of Volcanology, v. 57, p. 151–169.
Swisher, C. C., III, 1992, $^{40}Ar/^{39}Ar$ dating and its application to the calibration of the North American Land Mammal ages [Ph.D. thesis]: Berkeley, University of California, 239 p.
Trimble, D. E., 1976, Geology of the Machaud and Pocatello quadrangles, Bannock and Power counties, Idaho: U.S. Geological Survey Bulletin 1400, 88 p.
Van Houten, F. B., 1956, Reconnaissance of Cenozoic sedimentary rocks of Nevada: American Association of Petroleum Geologists Bulletin, v. 40, p. 2801–2825.
Warren, R. G., Byers, F. M., Jr., Broxton, D. E., Freeman, S. H., and Hagan, R. C., 1989, Phenocryst abundances and glass and phenocryst composition as indicators of magmatic environments of large-volume ash flow sheets in southwestern Nevada: Journal of Geophysical Research, v. 94, p. 5987–6020.
Wendell, 1970, The structure and stratigraphy of the Virgin Valley–McGee Mountain area, Humboldt County, Nevada [Master's thesis]: Eugene, University of Oregon, 130 p.
Whistler, D. P., and Burbank, D. W., 1992, Miocene biostratigraphy and biochronology of the Dove Spring Formation, Mojave Desert, California, and the characterization of the Clarendonian mammal age (late Miocene) in California: Geological Society of America Bulletin, v. 104, p. 644–658.
Williams, S. K., 1994, Late Cenozoic tephrostratigraphy of deep sediment cores from the Bonneville basin, northwest Utah: Geological Society of America Bulletin, v. 106, p. 1517–1530.

MANUSCRIPT RECEIVED BY THE SOCIETY AUGUST 5, 1996
REVISED MANUSCRIPT RECEIVED MAY 17, 1997
MANUSCRIPT ACCEPTED JULY 11, 1997

Printed in U.S.A.